國立交通大學

電信工程學系

碩士論文

心電圖訊號的渦漩和適應性多速率壓縮

Turbo and Adaptive Multirate Compressions of Electrocardiogram Signals

研 究 生：施泓瑋

指導教授：蘇育德　博士

西元 2006 年 9 月

心電圖訊號的渦漩和適應性多速率壓縮

Turbo and Adaptive Multirate Compressions of Electrocardiogram Signals

研究生：施泓瑋　　Student：Hong-Wei Shih

指導教授：蘇育德 博士　　Advisor：Dr. Yu T. Su

國立交通大學
電信工程學系碩士班
碩士論文

A Thesis Submitted to

Department of Communication Engineering

College of Electrical and Computer Engineering

National Chiao Tung University

In Partial Fulfillment of the

Requirements for the Degree of

Master of Science

In Communication Engineering

Hsinchu, Taiwan, Republic of China
September 2006

心電圖訊號的渦漩和適應性多速率壓縮

研究生: 施泓瑋　　　　　　　　　　　　　　　　　　指導教授: 蘇育德 博士

國立交通大學電信工程學系碩士班

中文摘要

本文提出兩種新型的心電圖訊號壓縮技術。第一種方式應用了迭代式(iterative)通道解碼的渦輪原理(turbo principle)，而第二種方式則借用了最新的標準語音編碼法，即適應性多速率寬頻編碼。後者可提供較佳的壓縮比但前者較適合於合併式的訊源通道編碼。

無失真的壓縮是透過將渦輪編碼器輸出加以適當的穿刺(puncture)後再經迭代式解碼還原。穿刺的比率會逐漸上升直到無法達到零失真還原爲止。因爲正交轉換可提供心電圖訊號一種有用的表示法，能夠很簡單的區隔數據的重要性，我們先用離散餘弦轉換(DCT)將心電圖數據轉換之後，再透過上述的渦輪壓縮過程，依轉換後數據之重要性來作穿刺，穿刺後的數據復利用渦輪（迭代式）解碼法去檢測訊源端的完整性和可回復性來確定資料源是可正確無誤的重建。爲避免壓縮後的數據因爲在傳輸過程遭到雜訊干擾無法正確解碼，我們可以在傳輸端加入部份原先穿刺掉的（通常是重要較高的部份）位元用來抵抗雜訊。這種合併訊源通道的編碼方式只需要單一的編解器，在解碼器也不需要訊源的參數（如其先驗機率分佈），即可從事迭代解碼。

除此之外，我們也利用所謂「適應性多速率寬頻編碼法」提出一種新穎的心電圖壓縮方法。「適應性多速率寬頻編碼法」在語音壓縮方面已經有很顯著的成功。我們修正了這種方法從另一種觀點來處理一維的心電圖訊源。我們是利用碼激勵線性預測(CELP)編碼爲基型(合成分析法)來作心電圖的編碼。首先，我們利用長時距預測濾波器(Long Term Predictor)得到心電圖訊號的近似週期和增益。心電圖訊號經長時距預測濾波器後的訊號會先通過短時距預測(Short Term Predictor)濾波器，再以後者的輸出建立碼簿(Codebook)。如此一來，我們只需傳送長時距預測濾波器和短時距預測濾波器的係數以及建立出來的碼簿的索引便可重建原始信號。電腦模擬的結果顯示這種方法對心電圖壓縮非常有效，在均方根誤差百分比約爲３%的要求下，可達到壓縮比率 30 左右。

Turbo and Adaptive Multirate Compressions of Electrocardiogram Signals

Student : Hong-Wei Shih　　Advisor : Yu T. Su

Department of Communication Engineering

National Chiao Tung University

Abstract

Several recent publications have shown that joint source-channel decoding could be a powerful technique. In the first part of this thesis, we propose the use of punctured turbo codes with the idea of unequal error protection (UEP) to perform lossless compression and joint source channel coding of ECG data using the discrete cosine transform (DCT), because orthogonal transforms provide alternate signal representations that can be useful for electrocardiogram (ECG) data compression. Compression is achieved by puncturing the turbo code to the desired rate. We use the turbo principle to iteratively estimate the source integration and to compensate the error due to compression. No information about the source distribution is required in the encoding processing. Moreover, the source parameters do not need to be known in the decoder, since that can be estimated jointly with the iterative decoding process. We also present an useful puncturing method, which ensures the compression of ECG data in a predetermined number of reconstruction attempts.

The second part of this thesis presents a novel approach for compression of ECG signals based on the adaptive multi-rate wideband codec method. Adaptive multi-rate wideband codec method has achieved prominent success in speech compression. Here we use a modified version of adaptive multi-rate wideband codec method for one dimensional signals. We applied adaptive multi-rate wideband codec method on different records of ECG signal database. Numerical experiments show that this method has a very high efficient compression performance. Using the percent-root-mean-square distortion (PRD) measure, the coder is shown to give a compression ratio about 30 with a PRD less than 3.0%.

Contents

List of Figures

Chapter 1

Introduction

Conventional source codes, e.g. Huffman codes or arithmetic codes, remove redundancy very efficiently and thus achieve compression rates very close the theoretical limit–the entropy rate of the source. However, these methods are very sensitive to errors such as those resulted from the re-synchronization process.

During the last decade, robust source coding techniques based on forward error correcting codes have been introduced. Approaches based on low-density parity-check (LDPC) codes were studied in [1], [2], whereas [3], [4] concentrated on source coding using turbo codes. Their common success relies on the usage of a probability-based message-passing algorithm during decoding.

It is well known that data compression and data transmission are essentially dual problems. In compression (source coding) we remove all the redundancy in the data to form the most compressed version possible whereas in transmission (channel coding) over noisy channels we add redundancy in a controlled fashion to combat errors in the channel.

Turbo codes form a class of very powerful channel codes that yield near-Shannon limit performance. The principle of turbo (iterative) decoding has been applied to areas other than channel codes. More recently, the turbo principle has been applied successfully to data compression of binary memoryless sources. Source coding schemes based on the turbo principle can be easily extended to obtain powerful joint source-channel codes for point-to-point transmission [5]. In the first part of this thesis we present a joint turbo source and channel coding scheme for ECG signals. The spectral property of ECG signals is used for designing puncture patterns for turbo compression and a compression ratio of 10 is achieved.

An apparent similarity between speech and ECG signals suggests that it is feasible to apply speech coding technologies to ECG data compression. The so-called Adaptive Multi-Rate Wideband (AMR-WB) method has been proved to be very efficient for speech coding and has been adopted as an industrial standard. The main idea is to compact the signal energy in much less samples than in the original wave samples. In the second part of this thesis, we report our findings about a modified AMR-WB approach for ECG data compression.

The outline of this thesis is as follows. In the ensuing section, we describe the strategy we adopted in presenting the existing ECG data compression schemes and introduce some properties about the ECG wave. The concepts of decremental redundancy and the associated decoding method are presented and our coding scheme is introduced in Section 3,. In Section 4, we provide detailed description of the Adaptive Multi-Rate Wideband codec algorithm and apply it for ECG signal compression.

Chapter 2

Electrocardiogram Data Compression Method

The main goal of any compression technique is to achieve maximum data volume reduction while preserving the significant signal morphology features upon reconstruction. A broad spectrum of techniques for electrocardiogram (ECG) data compression have been proposed during the last four decades. Such techniques have been vital in reducing the digital ECG data volume for storage and transmission. These techniques are essential to a wide variety of applications ranging from diagnostic to ambulatory ECG's. Due to the diverse procedures that have been employed, comparison of ECG compression methods is a major problem. Present evaluation methods preclude any direct comparison among existing ECG compression techniques. ECG data compression schemes are presented in two major groups: direct data compression and transformation methods. The direct data compression techniques are: ECG differential pulse code modulation and entropy coding, AZTEC, Turning-point, CORTES, Fan and SAPA algorithms, peak-picking, and cycle-to-cycle compression methods. The transformation methods briefly presented, include: Fourier, Walsh, and K-L transforms. The theoretical basis behind the direct ECG data compression schemes are presented and classified into three categories: tolerance-comparison compression, differential pulse code modulation (DPCM), and entropy coding methods.

Existing ECG data compression techniques have been developed and evaluated under different conditions and constraints. Independent databases, with ECG's sampled and digitized at different sampling frequencies ($100 - 1000$ Hz) and precisions ($8 - 12$ bits), have been mainly employed. The reported compression ratios (CR) have been strictly based on comparing the number of samples in the original data with the resulting compression parameters without taking into account factors such as bandwidth, sampling frequency, precision of the original data, wordlength of compression parameters, reconstruction error threshold, database size, lead selection, and noise level.

Each compression scheme is presented in accordance to the following five issues: a) a brief description of the structure and the methodology behind each ECG compression scheme is presented along with any reported unique advantages and disadvantages. b) The issue of processing time requirement for each scheme has been excluded. In light of the current technology, all ECG compression techniques can be implemented in real-time environments due to the relatively slow varying nature of ECG signals. c) The sampling rate and precision of the ECG signals originally employed in evaluating each compression scheme are presented along with the reported compression ratio. d) Since most of the databases utilized in evaluating ECG compression schemes are nonstandard, database comparison has been excluded. We believe such information does not provide additional clarity and at times may be misleading. However, every effort has been made to include comments on how well each compression scheme has performed. The intent is to give the reader a feeling for the relative value of each compression technique. e) Finally, the fidelity measure of the reconstructed signal compared to the original ECG has been primarily based on visual inspection. Besides the visual comparison, many compression schemes have employed the percent root-mean-square difference (PRD). The PRD value for each compression scheme is presented whenever it is available. The PRD calculation is as follows:

$$PRD = \sqrt{\frac{\sum_{i=1}^{n}[x_{org}(i) - x_{rec}(i)]^2}{\sum_{i=1}^{n} x_{org}^2(i)}} * 100 \tag{2.1}$$

where x_{org} and x_{rec} are samples of the original and reconstructed data sequences.

2.1 Introduction to Electrocardiogram (ECG)

An electrocardiogram (ECG or EKG, abbreviated from the German Elektrokardiogramm) is a graphic representation produced by an electrocardiograph, which records the electrical voltage in the heart in the form of a continuous strip graph. It is the prime tool in cardiac electrophysiology, and has a prime function in screening and diagnosis of cardiovascular diseases. An ECG is constructed by measuring electrical potential between various points of the body using a galvanometer. Leads I, II and III are measured over the limbs: I is from the right to the left arm, II is from the right arm to the left leg and III is from the left arm to the left leg. From this, the imaginary point V is constructed, which is located centrally in the chest above the heart. The other nine leads are derived from potential between this point and the three limb leads (aVR, aVL and aVF) and the six precordial leads (V_{1-6}).

Therefore, there are twelve leads in total. Each, by their nature, record information from particular parts of the heart:

- The inferior leads (leads II, III and aVF) look at electrical activity from the vantage point of the inferior region (wall) of the heart. This is the apex of the left ventricle.

- The lateral leads (I, aVL, V_5 and V_6) look at the electrical activity from the vantage point of the lateral wall of the heart, which is the lateral wall of the left ventricle.

- The anterior leads, V_1 through V_6, and represent the anterior wall of the heart, or the frontal wall of the left ventricle.

- aVR is rarely used for diagnostic information, but indicates if the ECG leads were placed correctly on the patient.

Understanding the usual and abnormal directions, or vectors, of depolarization and repolarization yields important diagnostic information. The right ventricle has very little muscle mass. It leaves only a small imprint on the ECG, making it more difficult to diagnose than changes in the left ventricle.

The leads measure the average electrical activity generated by the summation of the action potentials of the heart at a particular moment in time. For instance, during normal atrial systole, the summation of the electrical activity produces an electrical vector that is directed from the SA node towards the AV node, and spreads from the right atrium to the left atrium (since the SA node resides in the right atrium). This turns into the P wave on the EKG, which is upright in II, III, and aVF (since the general electrical activity is going towards those leads), and inverted in aVR (since it is going away from that lead).

A typical ECG tracing of a normal heartbeat consists of a P wave, a QRS complex and a T wave, is shown in Fig. 2.1. A small U wave is not normally visible.

1. Axis

   The axis is the general direction of the electrical impulse through the heart. It is usually directed to the bottom left (normal axis: -30^o to $+90^o$), although it can deviate to the right in very tall people and to the left in obesity.

   - Extreme deviation is abnormal and indicates a bundle branch block, ventricular hypertrophy or (if to the right) pulmonary embolism.

   - It also can diagnose dextrocardia or a reversal of the direction in which the heart faces, but this condition is very rare and often has already been diagnosed by something else (such as a chest X-ray).

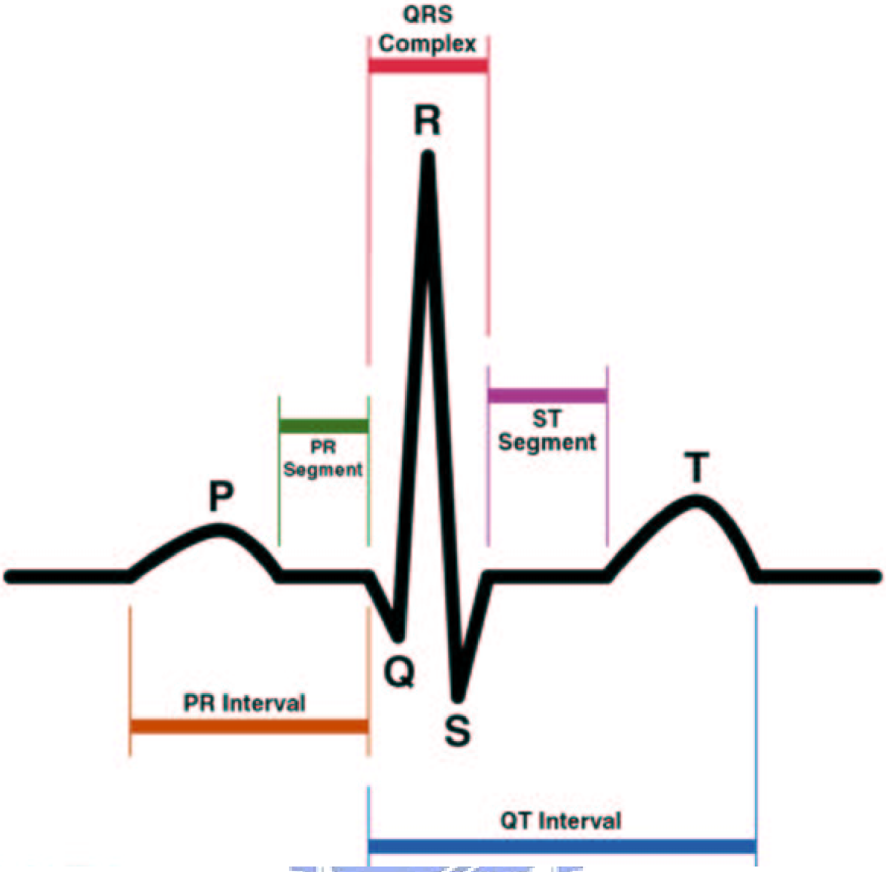

Figure 2.1: Schematic representation of normal ECG trace (sinus rhythm), with waves, segments, and intervals labeled

2. P wave

   The P wave is the electrical signature of the current that causes atrial contraction. Both the left and right atria contract simultaneously. Its relationship to QRS complexes determines the presence of a heart block.

   - Irregular or absent P waves may indicate arrhythmia.
   - The shape of the P waves may indicate atrial problems.

3. QRS

   The QRS complex corresponds to the current that causes contraction of the left and right ventricles, which is much more forceful than that of the atria and involves more muscle mass, thus resulting in a greater ECG deflection. The duration of the QRS complex is normally less than or equal to 0.10 second. The Q wave, when present, represents the small horizontal (left to right) current as the action potential travels through the interventricular septum.

- Very wide and deep Q waves do not have a septal origin, but indicate myocardial infarction that involves the full depth of the myocardium and has left a scar.

The R and S waves indicate contraction of the myocardium itself.

- Abnormalities in the QRS complex may indicate bundle branch block (when wide), ventricular origin of tachycardia, ventricular hypertrophy or other ventricular abnormalities.
- The complexes are often small in pericarditis or pericardial effusion.

4. *T* wave

The *T* wave represents the repolarization of the ventricles. The QRS complex usually obscures the atrial repolarization wave so that it is not usually seen. Electrically, the cardiac muscle cells are like loaded springs. A small impulse sets them off, they depolarize and contract. Setting the spring up again is repolarization (more at action potential). In most leads, the T wave is positive.

- Inverted (also described as negative) T waves can be a sign of disease, although an inverted T wave is normal in V1 (and V2-V3 in African-Americans/Afro-Caribbeans).
- T wave abnormalities may indicate electrolyte disturbance, such as hyperkalemia or hypokalemia.

The ST segment connects the QRS complex and the T wave.

- This segment ordinarily lasts about 0.08 second and is usually level with the PR segment. Upward or downward displacement may indicate damage to the cardiac muscle or strain on the ventricles. It can be depressed in ischemia and elevated in myocardial infarction, and upslopes in digoxin use.

5. *U* Wave

The *U* wave is not always seen. It is quite small, and follows the T wave by definition. It is thought to represent repolarization of the papillary muscles or Purkinje fibers. Prominent U waves are most often seen in hypokalemia, but may be present in hypercalcemia, thyrotoxicosis, or exposure to digitalis, epinephrine, and Class 1A and 3 anti-arrhythmics, as well as in congenital long QT syndrome and in the setting of intracranial hemorrhage. An inverted U wave may represent myocardial ischemia or left ventricular volume overload.

6. QT interval

The QT interval is measured from the beginning of the QRS complex to the end of the T wave. A normal QT interval is usually about 0.40 seconds. The QT interval as well as the corrected QT interval are important in the diagnosis of long QT syndrome and short QT syndrome. The QT interval varies based on the heart rate, and various correction factors have been developed to correct the QT interval for the heart rate. The most commonly used method for correcting the QT interval for rate is the one formulated by Bazett and published in 1920. Bazett's formula is $QT_c = \frac{QT}{\sqrt{RR}}$, where QTc is the QT interval corrected for rate, and RR is the interval from the onset of one QRS complex to the onset of the next QRS complex, measured in seconds. However, this formula tends to not be accurate, and over-corrects at high heart rates and under-corrects at low heart rates.

7. PR interval

The PR interval is measured from the beginning of the P wave to the beginning of the QRS complex. It is usually 0.12 to 0.20 seconds. A prolonged PR indicates a first degree heart block, while a shorting may indicate an accessory bundle that depolarizes the ventricle early, such as seen in Wolff-Parkinson-White syndrome.

2.2 Direct ECG Data Compression Schemes

This section presents the direct data compression schemes developed specifically for ECG data compression, namely, the AZTEC, Fan/SAPA, TP, and CORTES ECG compression schemes.

1. The AZTEC Technique: The amplitude zone - time epoch coding (AZTEC) algorithm originally developed by Cox et al. [6] for preprocessing real-time ECGs for rhythm analysis. It has become a popular data reduction algorithm for ECG monitors and databases with an achieved compression ratio of 10: 1 (500 Hz sampled ECG with 12 b resolution). However, the reconstructed signal demonstrates significant discontinuities and distortion. In particular, most of the signals distortion occurs in the reconstruction of the P and T waves due to their slow varying slopes. The AZTEC algorithm converts raw ECG sample points into plateaus and slopes. The AZTEC plateaus (horizontal lines) are produced by utilizing the zero-order interpolation (ZOI). The stored values for each plateau are the amplitude value of the line and its length (the number of samples with which the line can be interpolated within aperture ϵ). The production of an AZTEC slope starts when the number of samples needed to form a plateau is less than three. The slope is saved whenever a plateau of three samples or more can be formed. The stored values for the slope are the duration (number of samples of the slope) and the final elevation (amplitude of last sample point). Signal reconstruction is achieved by expanding the AZTEC plateaus and slopes into a discrete sequence of data points. Even though the AZTEC provides a high data reduction ratio, the fidelity of the reconstructed signal is not acceptable to the cardiologist because of the discon-

tinuity (step-like quantization) that occurs in the reconstructed ECG waveform. A significant reduction of such discontinuities is usually achieved by utilizing a smoothing parabolic filter. The disadvantage of utilizing the smoothing process is the introduction of amplitude distortion to the ECG waveform.

2. The Turning Point Technique: The turning point (TP) data reduction algorithm [7] was developed for the purpose of reducing the sampling frequency of an ECG signal from 200 to 100 Hz without diminishing the elevation of large amplitude QRS's. The algorithm processes three data points at a time; a reference point (X_0) and two consecutive data points (X_1 and X_2). Either X_1 or X_2 is to be retained. This depends on which point preserves the slope of the original three points. The TP algorithm produces a fixed compression ratio of 2 : 1 whereby the reconstructed signal resembles the original signal with some distortion. A disadvantage of the TP method is that the saved points do not represent equally spaced time intervals.

3. The CORTES Scheme: The coordinate reduction time encoding system (CORTES) algorithm [8] is a hybrid of the AZTEC and TP algorithms. CORTES applies the TP algorithm to the high frequency regions (QRS complexes), whereas it applies the AZTEC algorithm to the isoelectric regions of the ECG signal. The AZTEC and TP algorithms are applied in parallel to the incoming sampled ECG data. Whenever an AZTEC line is produced, a decision based on the length of the line is used to determine whether the AZTEC data or the TP data is to be saved. If the line is longer than an empirically determined threshold, the AZTEC line is saved, otherwise the TP data are saved. Only AZTEC plateaus (lines) are generated; no slopes are produced. The CORTES signal reconstruction is achieved by expanding the AZTEC plateaus into discrete data points and interpolating between each pair of the TP data. Parabolic smoothing is applied to AZTEC portions

of the reconstructed CORTES signal to reduce distortion. Detailed description of the CORTES implementation and reconstruction procedures are discussed in Tompkins and Webster [9]

4. Fun and SAPA Techniques: Fan and scan-along polygonal approximation (SAPA) algorithms, developed for ECG data compression, are based on the first-order interpolation with two degrees of freedom (FOI-2DF) technique. A recent report [10] claimed that the SAPA-2 algorithm is equivalent to an older algorithm, the Fan.

2.3 Transformation ECG Data Compression Schemes

Unlike direct data compression, most of the transformation compression techniques have been employed in ECG or multilead ECG compression and require ECG wave detection. In general, transformation techniques involve preprocessing the input signal by means of a linear orthogonal transformation and properly encoding the transformed output (expansion coefficients) and reducing the amount of data needed to adequately represent the original signal. Upon signal reconstruction, an inverse transformation is performed and the original signal is recovered with a certain degree of error. However, the rationale is to efficiently represent a given data sequence by a set of transformation coefficients utilizing a series expansion (transform) technique. Many discrete orthogonal transforms have been employed in digital signal representation such as Karhunen-Loeve transform (KLT), Fourier (FT), Cosine (CT), Walsh (WT), Haar (HT), etc. The optimal transform is the KLT (also known as the principal components transform or the eignevector transform) in the sense that the least number of orthonormal functions is needed to represent the input signal for a given rms error. Moreover, the KLT results in decorrelated transform coefficients (diagonal covariance matrix) and minimizes the total entropy compared to any other transform. However, the computational time needed to calculate the KLT basis vectors (functions) is very intensive. This is due to the fact that the KLT basis vectors are based on determining the eigenvalues and corresponding eigenvectors of the covariance matrix of the original data, which can be a large symmetric matrix. The lengthy processing requirement of the KLT has led to the use of suboptimum transforms with fast algorithms (i.e., FT, WT, CT, HT, etc). Unlike the KLT, the basis vectors of these suboptimum transforms are input-independent (predetermined). For instance, the basis vectors in the FT are simply sines and cosines (fundamental frequency and multiples thereafter), whereas the WT basis vectors are square waves of different sequences. It should be pointed out that the performance of these suboptimal transforms is usually upper-bounded by the one of the KLT.

Orthogonal transforms provide alternate signal representations that can be useful for ECG data compression. The goal is to select as small a subset of the transform coefficients as possible which contain the most information about the signal, with introducing objectionable error after reconstruction. A more adaptive method which we proposed is to calculate the upper bound in the spectrum and keep the coefficients that contain a predetermined fraction of this power. The method is attractive because it can adapt to store more or less coefficients as necessary. This is a particularly useful feature for ambulatory systems where good compression under a variety of ECG rhythms is desirable.

2.4 Transform Representation

Orthogonal transforms provide alternate signal representations that can be useful for ECG data compression. Fig. 2.2, show an input signal with a sampling rate of 977 points/second and in Fig. 2.3 the discrete cosine transform of an electrocardiogram signal is given; it is clear from this diagram that the majority of the power in the transform is generally contained within the first 100 of the 1024 coefficients. Although a compression ratio of 10 : 1 with very little distortion might seem possible, this is not the case. The compression algorithm must also determine a threshold for how many

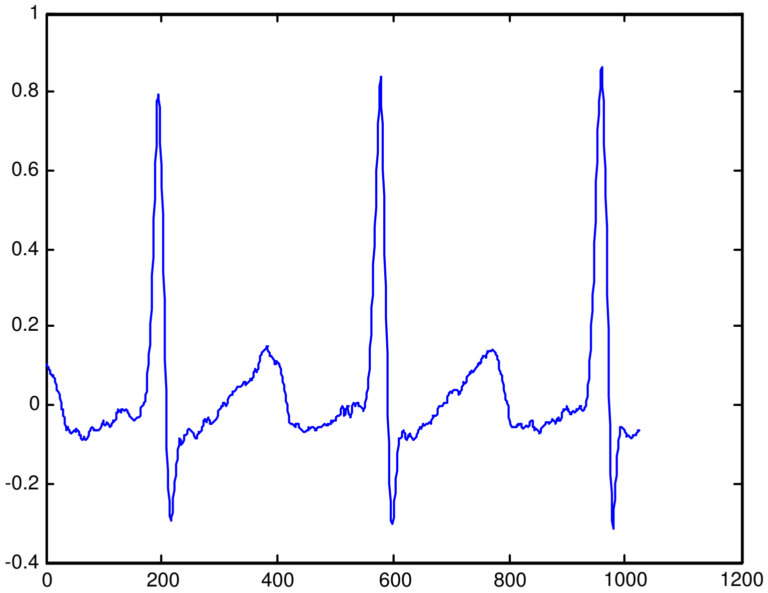

Figure 2.2: Input signal

coefficients are stored at their original accuracy. There are two methods to do this, the first and simpler is to fix the number of data points kept e.g. first 20% of coefficients retained at original accuracy. The vast majority of the power in the transform will be contained in these coefficients. A more adaptive method we proposed is to determine the upper bound in the spectrum and use it as the threshold to keep the coefficients that contain the vast majority of the power.

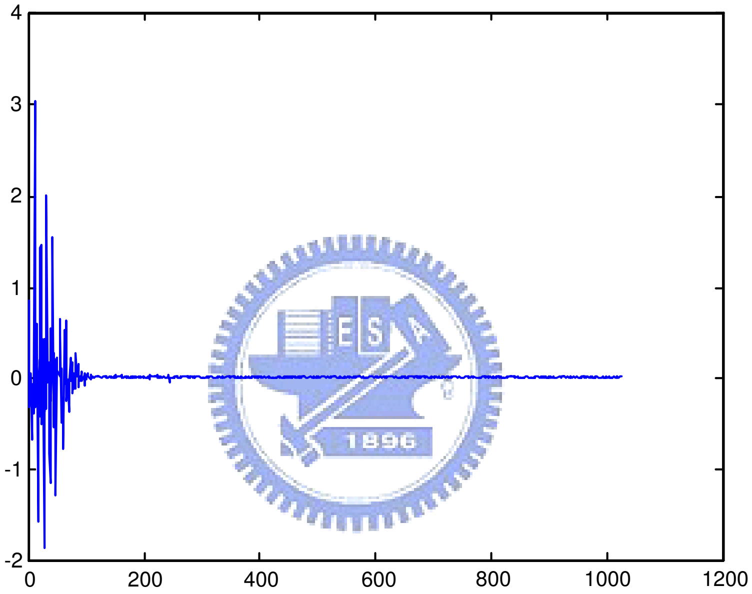

Figure 2.3: Signals spectrum after discrete cosine transform.

Chapter 3

Joint Turbo Source and Channel Coding

It is well known that data compression and data transmission are essentially dual problems. In compression we remove all the redundancy in the data to form the most compressed version possible-the focus of source coding-whereas in transmission over noisy channels we add redundancy in a controlled fashion to combat errors in the channel-the purpose of channel coding. In the past decade a series of research breakthroughs in the field of channel coding (most notably [11]), have rendered a large number of coding schemes which can achieve near-to-optimal performance (i.e. very close to channel capacity) with reasonable complexity. The secret of their success lies in the use of a 'turbo' feedback in an iterative decoding scheme, an ingenious approach we call the 'turbo principle' [12]. More recently, the turbo principle has been applied successfully to data compression of binary memoryless sources [13]. While in [14] the objective is to improve the error correction after transmission over a channel and therefore all encoded bits are useful, in the dual source coding problem addressed in [13] there is no channel involved and so the encoded bits can be punctured heavily depending on the desired compression rate. An alternative scheme based on LDPC codes and belief propagation decoding was presented in [1].

3.1 Decremental Redundancy–Source Coding

Let U be a binary, memoryless source drawn i.i.d. with $p_0 = P(U = 0)$. In this section we describe how to encode a source block $U^N = (u_1, \cdots, u_n, \cdots, u_N)$ of length N resulting in a binary codeword X^K. We state how to generate this codeword in order to achieve compression on the one hand and protect the source information against channel impairments on the other hand. Our discussion can be expanded to any binary source.

We use log-likelihood values with the natural logarithm throughout our discussion. For discrete model $y = x + n$, where y is the sample at the output of the received baseband matched filter, and $x \in \{0, 1\}$ is the transmitted signal, we define the source state information (SSI) and the channel state information (CSI) by the two log-likelihood ratios

$$L_S = \log \frac{p_0}{1 - p_0}, \quad L(y|x) = \log \frac{p(y|x = 0)}{p(y|x = 1)} = L_C \cdot y$$

$L_C = 4E_s/N_0$ for an additive white Gaussian noise (AWGN) channel and it is either ∞ or 0 for the binary erasure channel (BEC). In turbo source coding we successively remove the redundancy of a source sequence to obtain its most compressed representation. As long as the rate of the source code, defined as $R_s = \frac{K}{N}$, is larger than the entropy of the source $H(U)$, the source block can be perfectly reconstructed (source coding theorem).

The proposed source coding scheme is based on the idea shown in Fig. 3.1. We briefly explain its operation in the following. Further details are shown in [4]. The task of turbo compression is to map a source sequence U^N to the compressed sequence X^K.

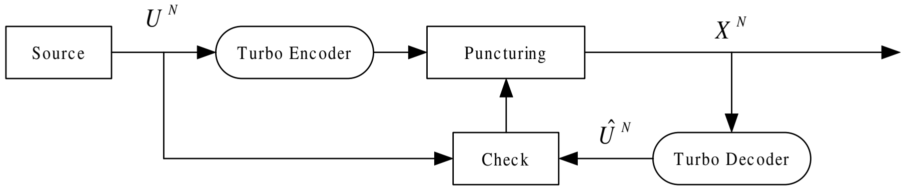

Figure 3.1: Lossless compression of a source block using turbo codes. Compression is achieved by puncturing and verifying the integrity of the reconstructed source sequence.

The decremental redundancy algorithm encodes a source block of a binary memoryless source using a parallel concatenated (PCC) turbo code. The constituent codes of the turbo code are rate one convolutional codes (or scramblers). The PCC coding scheme is depicted in Fig. 3.2 As stated in [3] compression should be achieved by randomly puncturing the scrambled (resp. parity) bits. In order to recover the source sequence perfectly, the randomly chosen puncturing pattern has to be saved. Accordingly, the side information is as long as the source block and thus compression is not possible. Hagenauer *et al.* [4] proposed this equivalent puncturing strategy depicted in Fig. 3.3

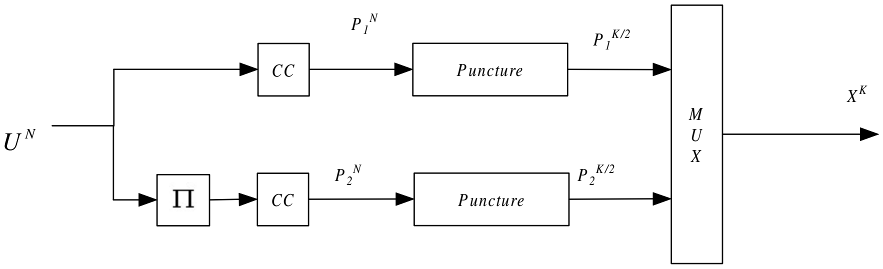

Figure 3.2: A parallel concatenation of rate 1 convolutional codes (CC) with an interleaver between them followed by heavy puncturing can be used to perform data compression of binary sources.

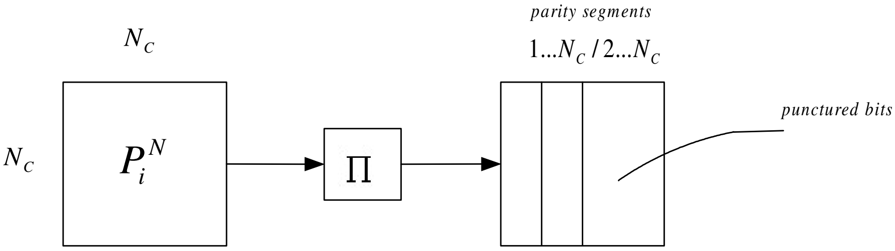

Figure 3.3: Puncturing scheme for decremental redundancy.

Each parity sequence is interleaved, written line by line into a square matrix and the bits are erased columnwise. The decremental redundancy algorithm for turbo source encoding, which has the following steps:

1. Let $i = N_c/2$

2. Encode the source block with a turbo encoder and store the output block.

3. Puncture the encoded block using i parity segments.

4. Decode the compressed block.

5. Check for errors. If the decoded block is error free, let $i = i + 1$ and go to step 3.

6. Let $i = i - 1$. Repeat 3, include a binary codeword corresponding to the index i, and stop.

Notice that the number of iterations required to find the best puncturing rate can be considerably reduced, if we store a table with different starting points for the optimization algorithm, depending on the probability distribution of the source. Since the sequences produced by the source are likely to be typical the number of iterations required to fine tune the compression rate will in general be small. We can also turn to a more sophisticated segmentation of the parity matrix, depending on the desired puncturing step.

Consequently, only the index of the last punctured column has to be known to reconstruct the source block. Since at least half of the parity bits have to be erased (otherwise we would have no compression) only $\lceil log_2(\sqrt{N}/2) \rceil$ bits have to be stored as side information to indicate the size of the actual codeword. Finally, the compressed codeword X^K is decoded using a parallel concatenated turbo decoder, resulting in the recovered source sequence $\hat{U}^N$. As long as the reconstructed sequence is identical to the source sequence, we further can remove redundancy. If the integrity test fails for the first time, the index of the last cancelled column is incremented by one, and the resulting non-punctured parity bit constitute the compressed data.

Further on, we have to remark that each APP decoder is modified in order to benefit from the source statistics of the non-uniformly distributed binary source. In duality to the channel state information in channel coding, this additional input to the decoder is called source state information. Thus APP component decoder is fed with the log-likelihood ratio $L_C \cdot y$, source state information L_S and a priori information L_A from the other component decoder. In turbo compression the communication channel is BEC.

3.2 Source Decoding

At first glance, random puncturing of bits does not seem to be a very sophisticated way of performing source compression. However, just as in channel coding with turbo codes, the sophisticated part lies in the use of a turbo decoder. The turbo decoder for our system is depicted in Fig. 3.4 We will use L-values to describe the values input and passed around by the turbo decoder. Given a binary random variable U, where for convenience $u \in +1, -1$, then the L-values is defined as,

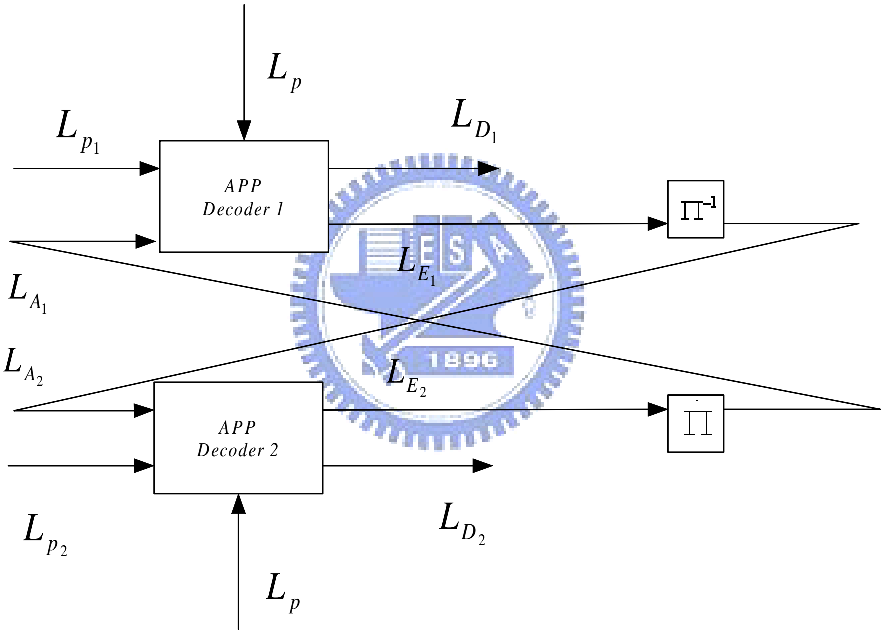

Figure 3.4: Parallel turbo source decoder.

$$L(U) = log_e \frac{P(u = +1)}{P(u = -1)}. \tag{3.1}$$

More details on L-values can be found in [15]. In Fig. 3.4, $L_{P_1}, L_{P_2}, L_{D_1}, L_{D_2}, L_{A_1}, L_{A_2}, L_{E_1}, L_{E_2}$ represent sequences of L-values. The letters A and E stand for "apriori" and "extrinsic" respectively. Since the parity bit sequences $P_1^{K/2}$ and $P_2^{K/2}$ can be thought of as being "transmitted" through a binary erasure channel (i.e. punctured), the corresponding input sequences L_{P_1} and L_{P_2} take on the L-values $\pm\infty$ (perfectly known bits) or 0 (erased).

In the case of a non-uniform binary source with $P(U = +1) = p$ and $P(U = -1) = 1 - p$, for which $H(U) = H_b(p)$ ((i.e. the binary entropy function), each decoder has an additional input vector L_P, where each element of the vector is equal to $L_p = log_e \frac{p}{1-p}$. We call this 'source' apriori knowledge and distinguish between apriori knowledge which is learnt during the iterations of the decoder which we will call 'learnt' apriori knowledge. In the case of more sophisticated (Markov) source models our source apriori vector would contain different sets of L_p values. The decoding algorithm is carried out according to Fig. 3.4. APP decoder 1 uses L_{P_1} and L_{A_1} (initialized to zero in the first iteration) to calculate the extrinsic L-values $L_{E_1} = L_{D_1} - L_{A_1} - L_P$. The sequence L_{E_1} is interleaved and passed onto APP decoder 2 as 'learnt' a priori knowledge L_{A_2}. Decoder 2 performs analogous operations and the process is then "iterated" until convergence is achieved.

3.3 Designing the Puncture Table: A Dual of Unequal Error Protection

In some analogue source coding applications, like speech or video compression, the sensitivity of the source decoder to errors in the coded symbols is typically not uniform: the quality of the reconstructed analogue signal is rather insensitive to errors affecting certain classes of symbols, while it degrades sharply when errors affect other classes. We assume that the source encoder produces frames of binary symbols. Each frame can be partitioned into classes of symbols of different 'importance' (i.e. of different sensitivity). Each importance class is associated to its bit error rate (BER) requirement. For fixed code rate, decoding delay and complexity, it is apparent that the best coding strategy, called unequal error protection (UEP) aims at achieving lower BER levels for the important classes while admitting higher BER levels for the unimportant ones. On the contrary, codes for which BER is (almost) independent of the position of the information symbols, are referred to as equal error protection (EEP) codes.

Turbo codes with UEP: Usually, turbo codes are punctured by using uniform puncturing patterns. In the following section we show that this approach leads to EEP turbo codes. Suppose now that the information symbols in U are partitioned into c classes, according to some importance criterion, and let k_l, denote the size of each class. Without loss of generality, we enumerate the classes in non-decreasing importance order. Moreover, we assume $k_1 < k_2 < \cdots < k_c$, as in usual speech and video coding applications. The intuitive idea for achieving UEP is as follows: we should increase the number of redundancy symbols correlated with the most important input symbols and reduce the redundancy correlated with the least important symbols, while keeping the total redundancy constant. This will be obtained by matching the puncturing patterns to the interleaver.

Then UEP is accomplished as follows: (i) arrange the input symbols u by rows in a $N_c \times N_c$ array U and consider a row-column interleaver, since it allows a clear graphical representation of the input symbols arrangement and of the puncturing patterns as $N_c \times N_c$ array, such that $N = N_c^2$ where N is the block size. (ii) each lth importance class is associated to a partial rate r_l, denoted as the inverse of the average number of turbo encoded output symbols per input symbol belonging to the lth class. (iii) Partition U into c disjoint sets S_l of positions (i, j) of size k_l , each corresponding to class l, respectively. (iv) finally, $\forall l = 1, \cdots, c$, a puncturing pattern realising the partial rate r_l is associated to the positions of S_l.

The choice of the position sets S_l, affects the UEP property of the resulting turbo code. In general, S_l must be chosen in order to correlate the turbo encoded redundancy symbols to the input symbols belonging to a class l.

The input symbols are arranged in a $N_c \times N_c$ array. An example of a good selection of the position subsets S_l is given in Table 3.1, where each position marked by l belongs to S_l for $l = 1, 2, 3$.

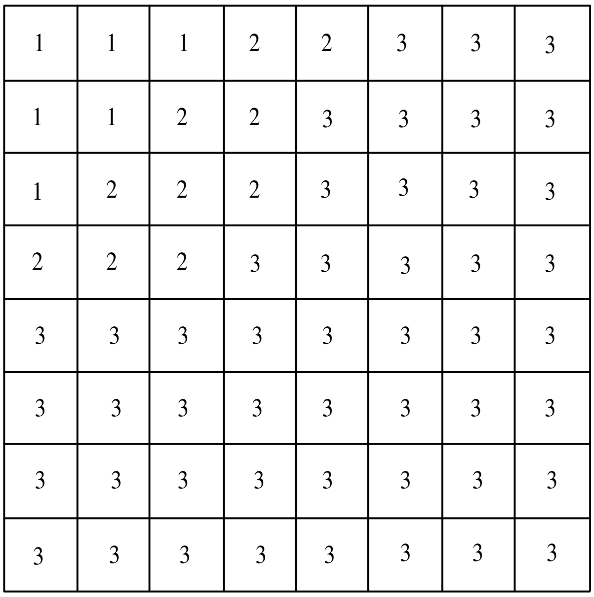

1	1	1	2	2	3	3	3
1	1	2	2	3	3	3	3
1	2	2	2	3	3	3	3
2	2	2	3	3	3	3	3
3	3	3	3	3	3	3	3
3	3	3	3	3	3	3	3
3	3	3	3	3	3	3	3
3	3	3	3	3	3	3	3

Table 3.1: Position subsets S_1, S_2, S_3

For the EEP design case we use uniform puncturing on the whole set of redundancy symbols. For the UEP design case, Table 3.2 shows a choice for the puncturing pattern p_1 (represented as a 13×13 binary array) which realises the partial rates for each class.

3.4 Upper Bounds of Discrete Cosine Transform

Application of fast discrete orthogonal transforms with various basis functions for data compression and efficient signal coding occupies a special place in the evolution of spectral representations. The digital spectral transform method is the main compression tool in various signal and image processing applications. Particularly, the discrete cosine transform (DCT) based compression algorithms have become industry standard (JPEG, MPEG) for still and video image compression systems. The following basic lemma supplies a method for computing the exact values of the upper bounds of spec-

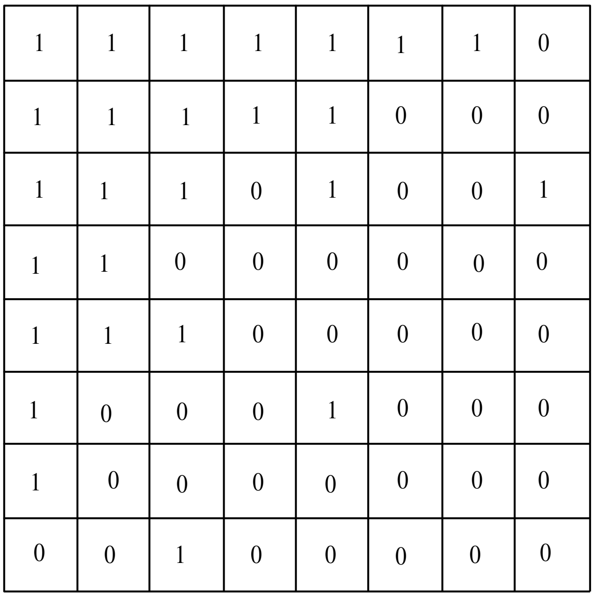

1	1	1	1	1	1	1	0
1	1	1	1	1	0	0	0
1	1	1	0	1	0	0	1
1	1	0	0	0	0	0	0
1	1	1	0	0	0	0	0
1	0	0	0	1	0	0	0
1	0	0	0	0	0	0	0
0	0	1	0	0	0	0	0

Table 3.2: Puncturing pattern p_1 for UEP code

tral coefficients' moduli on the class ω_Δ [16] where

$$\omega_\Delta = \{\overrightarrow{x} = (x_0, x_1, \cdots, x_{N-1}) : \max_{1 \le i \le N-1} |x_{i-1} - x_i| \le \Delta\}, \Delta > 0. \tag{3.2}$$

where $\vec{x}$ is the data vector.

Lemma 1 *Let $W = \| \omega_j(i) \|_{j,i=0}^{N-1}$ be the matrix of a real-value discrete orthogonal transform that satisfies the condition:*

$$\sum_{i=0}^{N-1} \omega_j(i) = 0, \;\; j = 1, 2, \cdots, N-1, \tag{3.3}$$

and $\overrightarrow{y} = W\overrightarrow{x} = (y_0, \cdots, y_{N-1})^T$. Then

$$\max_{\overrightarrow{x} \in \omega_\Delta} |y_j| = \Delta \cdot \sum_{m=1}^{N-1} \left| \sum_{i=0}^{m-1} \omega_j(i) \right|, \;\; j = 1, 2, \cdots, N-1. \tag{3.4}$$

The proof of this lemma is based on the known *dynamic programming principle* [17], that is the initial extremal task is being broken down into a multiple-step process and the extremum being sought at each step according to the *optimally principle.* Note, that conditions (3.3) are satisfied for most of classical *trigonometric, Walsh,* as well as

Haar transforms [16]. On the other hand the relationship (3.4) remains true without conditions (3.3) if we put $\overline{\omega}_\Delta$ instead of ω_Δ, where $\overline{\omega}_\Delta = \overrightarrow{x} \in \omega_\Delta, x_0 = 0$

In Fig. 3.5 the absolute value of DCT of an signal and it's DCT upper bound are given. By Fig. 3.5, we can set the threshold to keep the coefficients that contain the vast majority of the power in the spectrum.

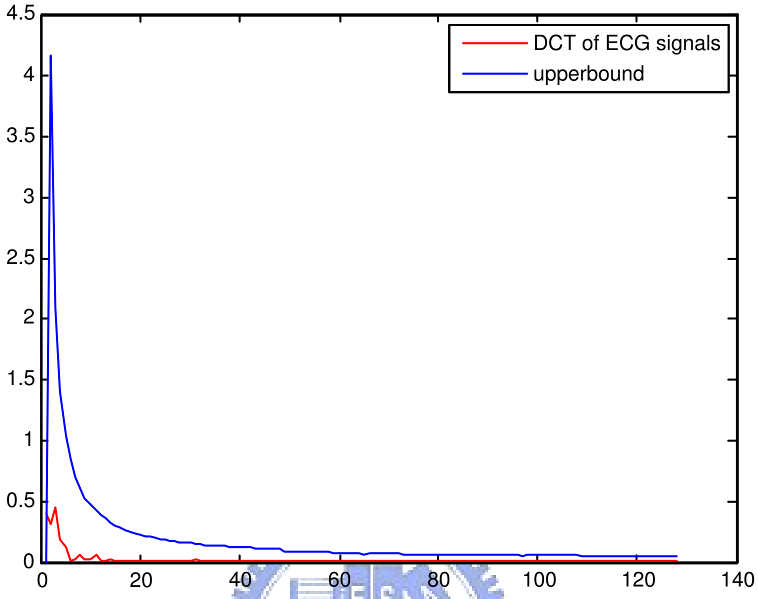

Figure 3.5: Signals spectrum after discrete cosine transform.

But in some cases, as in Fig. 3.6 the threshold may not so good in keeping the vast majority of the power in the spectrum. So we must use the UEP's idea to divide the different parts of the spectrum into different classes.

3.5 Joint Source and Channel Coding Using Unequal Protection

In this section, we present a joint source and channel coding method for electrocardiogram (ECG) signals based on transform data and unequal protection. This proposed compression scheme may find applications in digital Holter recording, in ECG signal

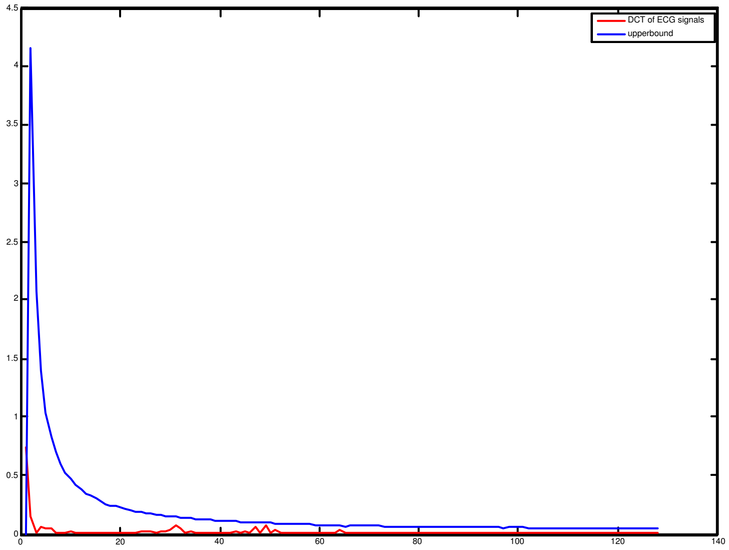

Figure 3.6: Signals spectrum after discrete cosine transform.

archiving and in ECG data transmission through communication channels. Using the new method, a compression ratio of 10 to 1 can be achieved with $PRD = 3.8\%$, in contrast to the AZTEC compression ratio of 6.8 to 1 with $PRD = 10.0\%$, the fan algorithm compression ratio of 7.4 to 1 with $PRD = 8.7\%$, and symmetric wavelet transform compression ratio of 8 to 1 with $PRD = 3.9\%$.

A turbo ECG compression system is shown in Fig. 3.7. The signal is first divided into

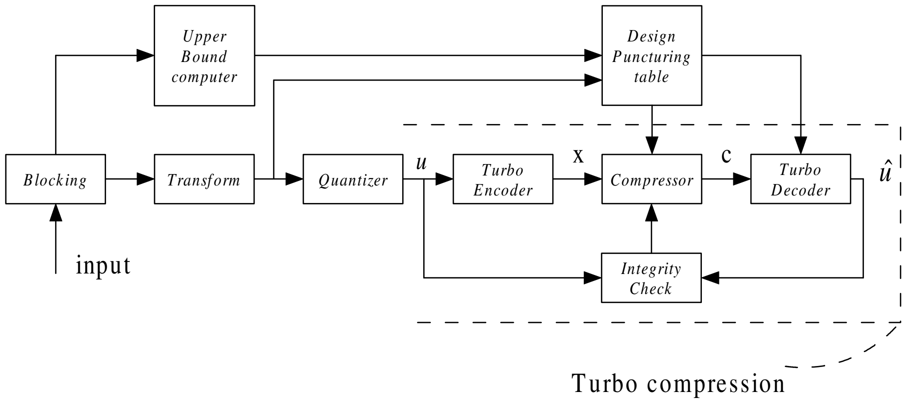

Figure 3.7: Block diagram of turbo-principle-based ECG compression

segments of n samples by a blocking algorithm. The segments are transformed using a Direct Cosine Transform. The upper bound computer determines the Δ in each blocks. Based on the Δ, the puncturing table could be designed by our puncturing scheme. The turbo compression scheme efficiently codes the output in the form of compressed data.

Detailed operations of each block are described below.

Blocking: The size of segmentation is important in determining the compression ratio and the distortion amplitude. A large number of points in a segment tends to increase the maximum of the upper bound, it makes the upper bound unreliable. We experimented with several segment sizes. For most ECG tapes, a block size of 1024 samples (1 seconds of record, about 2 normal beats) is appropriate.

Block size is an important issue about the system complexity. We used the discrete cosine transform to implement the transform block. So $O(NlogN)$ operations are needed for block size N of DCT. We choose N as small as possible to reduce the complexity of system. But the block size must keep the idea of transform method, it should have more than one normal beat period (about 350 to 450 samples).

1896

The performance of turbo code is effected by some factors, such as constrain length, iteration number, the size of interleaver, the category of interleaver ,and so on. The constrain length is usually $3 \sim 5$. Too large constrain length will increase the necessary decoding time and the complexity of decoding, but the improved effect of performance is limited. Here we will not discuss the influence of constrain length and iteration on the performance of turbo code. we only discuss on the effects of interleaver block size.

- Memory : Memory usage(interleaver size, extrinsic information registers, operation registers, $\cdots$) is directly proportion to the block size. So, the block size is choosed as small as possible to reduce the memory usage.

- Processing Time : The puncture scheme we proposed shows that decoding time is directly proportion to the block size, because of the turbo decoder's iteration times. So, the block size is choosed as small as possible to reduce the processing time.

- Performance : The greater block size N represents the better performance of turbo code. However, the drawback of great size is that increase the necessary of decoding time.

Transform: We used the discrete cosine transform to implement the transform block.

Upper bound computer: This is an important operation in the system. The number of bits assigned to the puncturing table is inversely proportional to the distortion at the reconstructed output. The objective is to count the best threshold to minimize the puncturing table's bit.

Quantizer: The quantizers is designed to uniformly round up the decomposed signals into integer values. Although a non-uniform quantizer will reduce the rate of distortion, it will cause a significant peak amplitude variation of the QRS complexes in the ECG signal.

Design Puncturing Table: In a first step the parity bits in each block P_i^N with $i = 1, 2$ are written line by line in a matrix $N_c \times N_c$, such that $N = N_c^2$, where N is the block size. since it allows a clear graphical representation of the input symbols arrangement and of the puncturing patterns. Second, based on the output from transform, a good selection of the position subsets S, is given in Table 3.3 , where each position marked by 1 belongs to S_l, for $l = 1, 2, 3$.

Third, based on the upper bound's output, we design the puncturing table could that achieve the compression rate desired shown in Table 3.4. To gradually remove the redundancy in the encoded stream we can eliminate one such parity segment at a time (in parallel for P_1^N and P_2^N), yielding a puncturing step of $2N_c/N$ that allows us to fine tune the compression rate. To make sure that the erased bits are spread out in the block we interleave the parity bits before puncturing them.

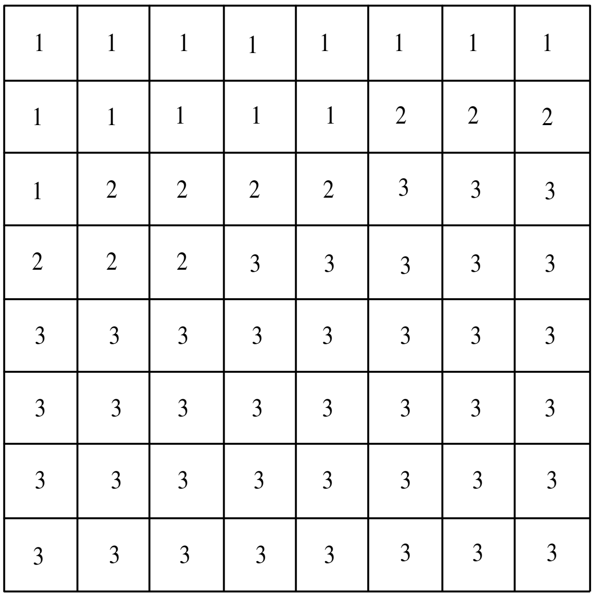

1	1	1	1	1	1	1	1
1	1	1	1	1	2	2	2
1	2	2	2	2	3	3	3
2	2	2	3	3	3	3	3
3	3	3	3	3	3	3	3
3	3	3	3	3	3	3	3
3	3	3	3	3	3	3	3
3	3	3	3	3	3	3	3

Table 3.3: Position subsets

Turbo compression: Turbo encoder is shown in Fig. 3.8. The only difference between traditional turbo code is our encoder without having the systemic part. The key idea of lossless compression is the puncturing table we proposed . We propose the decremental redundancy scheme illustrated in Fig. 3.4. The reconstructed source sequence is compared with the original block at the encoder side and the puncturing rate is adjusted to the result of this integrity test. This rate is decreased if the integrity test fails and vice versa. Puncturing , decoding, the check for integrity and rate adjustment defined as one cycle of the analysis by synthesis (AbS) loop. In each successful AbS loop, it depends on the convergence of the decoding algorithm which means we puncture less bits than it can be corrected by the chosen turbo code. Clearly, without convergence of the decoding result the source information cannot be perfectly recovered. To guarantee that the decoder is able to decode the input sequence without errors (lossless source coding), we can enable the encoder to test the decodability of its output. Since we want to achieve as much compression as possible, we puncture the parity bits on a step by step basis (decremental redundancy) as long as the compressed block can still be

1	1	1	1	1	1	1	0
1	1	1	1	1	0	0	0
1	1	1	0	0	0	0	0
1	1	0	0	0	0	0	0
1	0	0	0	0	0	0	0
0	0	0	0	0	0	0	0
0	0	0	0	0	0	0	0
0	0	0	0	0	0	0	0

Table 3.4: Puncturing pattern based on the upper bound computer, for UEP code

decoded error free by the test decoder at the source compression side. We now proceed to describe our decremental redundancy algorithm for turbo source encoding, which has the following steps:

1896

1. Let $i = N_c/2$.

2. Encode the source block with an encoder based on turbo principle and store the output block.

3. Puncture the encoded block using the idea of UEP.

4. Decode the compressed block.

5. Check for errors. If the decoded block is error free, let $i = i - 1$ and go back to step 3.

6. Let $i = i+1$. Repeat step 3, include a binary codeword corresponding to the index i , and stop.

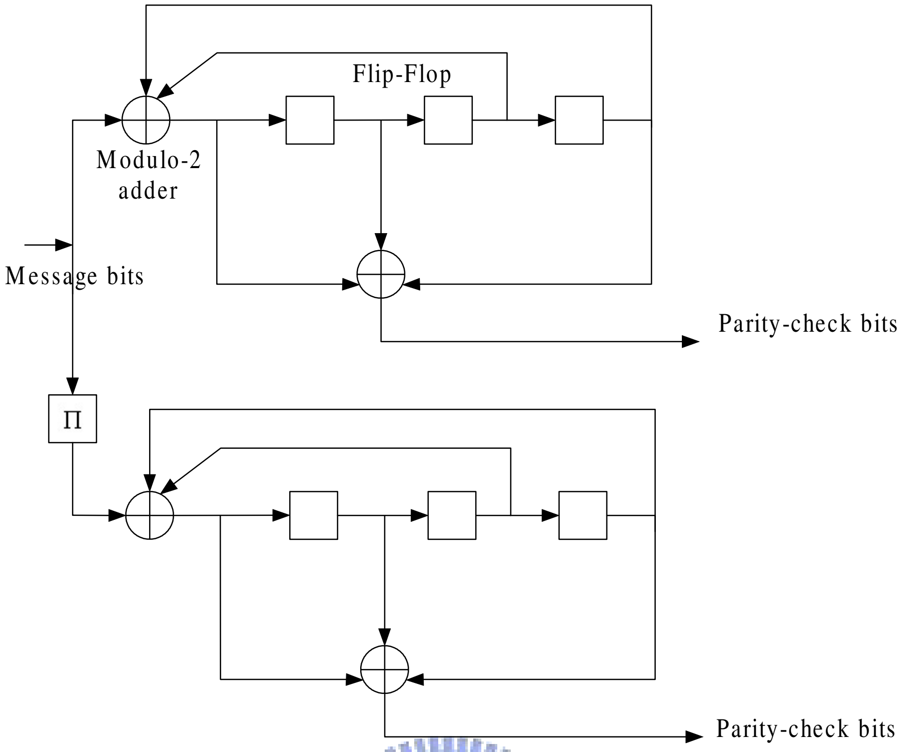

Figure 3.8: Block diagram of turbo-principle-based encoder

3.5.1 Simulation Results

The turbo compression method was applied to the ECG signal and transmit through Additive White Gaussian Noise (AWGN) channel. The results show the high efficiency of this method for ECG compression. The original signal, reconstructed signal and error between them for three records with the corresponding CR and PRD values are shown in Fig.3.9.

The compression ratios and the percent root-mean-square differences are tabulated below for the proposed method. Although the percent root-mean-square difference does not account for differences between morphology of two signals an may not report shape distortions, is used widely in signal compression literature as a standard measurement, because it is easy to compute and compare. Compression ratio (CR) is computed from the ratio of the original signals' samples (in bits) to the length of output bit stream. By

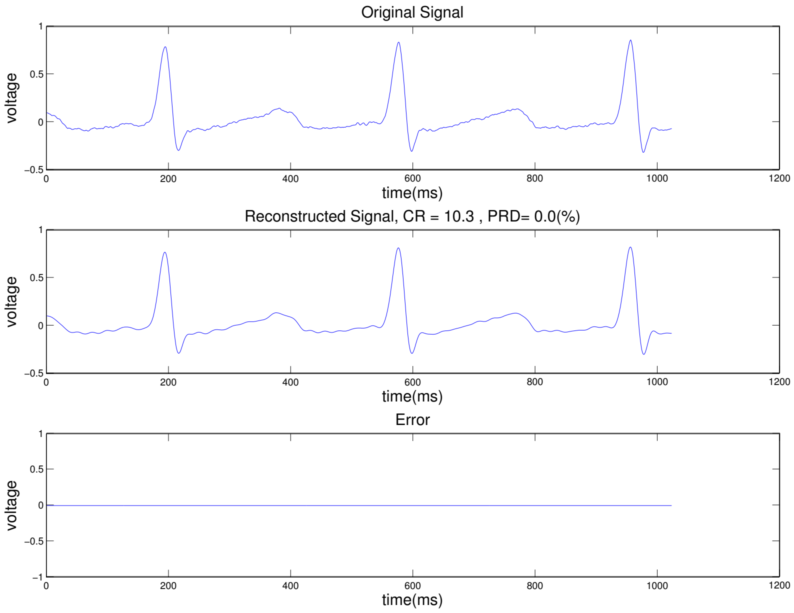
Original Signal

Reconstructed Signal, CR = 10.3 , PRD= 0.0(%)

Error

Figure 3.9: Compression with joint turbo source and channel coding

this method, we achieved the compression ratio about 10 with lossless data compression. Also , in table 3.5 is given the CR and PRD values for some other compression methods.

In Fig. 3.10, it shows that the proposed method has lower average PRD through an AWGN channel. The $SNRo$ defined as the ratio of the average power of the message signal (before compression) to the average power of the noise, both measured at the receiver output.

Compression method	Compression ratio	PRD (%)
AZTEC[6]	6.8	10.0%
TP[7]	2.0	5.3%
CORTES[8]	4.8	7.0%
Fan/SAPA[10]	3.0	4.0%
Symmetric Wavelet	7.9	3.9%
Proposed method	10.0	0.0%

Table 3.5: Compression performance for ECG signals with different compression method

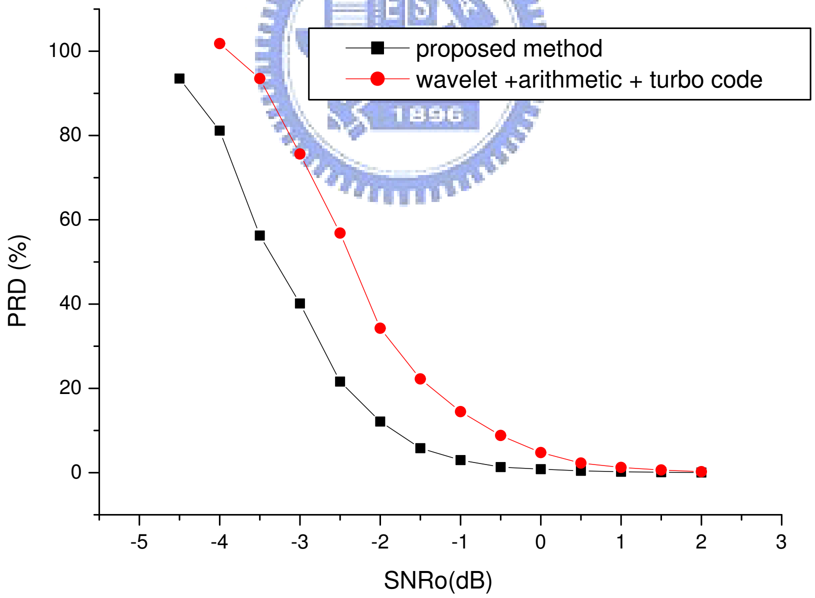

Figure 3.10: Average PRD comparison between proposed method and wavelet transform with arithmetic coding and rate-1/2 turbo coding

Chapter 4

Adaptive Multirate Approach for Electrocardiogram Compression

By inspection, there is an apparent similarity between speech and the nature of ECG signals, which indicates a possible application of speech coding technology to ECG data compression. There can be a large variance amongst different ECG's, reminiscent of that found in human speech. The importance of details in different rhythms varies over various applications while the ultimate goal is a coding algorithm that faithfully reproduces original signals.

The AMR-WB speech codec algorithm was selected in December 2000 and the corresponding specifications were approved in March 2001. The AMR-WB codec was also selected by the International Telecommunication Union-Telecommunication Sector (ITU-T) in July 2001 in the standardization activity for wideband speech coding around 16 kb/s and was approved in January 2002 as Recommendation G.722.2.

With the ultimate aim of using the idea of Adaptive Multi-Rate Wideband speech codec, the present thesis is structured as follows. The following section reviews the theoretical background of linear prediction and introduces the basic concepts of analysis-by-synthesis based linear predictive coders, the general class to which the Code-Excited Linear Prediction [18] coding algorithm belongs. Pitch prediction techniques and codebook constructed methods are also discussed.

4.1 The Code Excited Linear Prediction Coder

The proposed coder is based on the code excited linear prediction coder (CELP) structure for signal compression. CELP is a parametric coder; the basic parts comprise an excitation signal drawn from a codebook (a collection of codevectors) and shaped through a long term predictor and an AR filter (LPC model), synthesizing the output signal. The parameters are calculated in an analysis-by-synthesis fashion: the long-term and short-term filters ($l/P(z)$ and $l/A(z)$) are determined from the incoming signal, and the best codevector (in an MSE sense) is found through filtering, comparison, and selection.

The basic CELP is shown in Fig.4.1. Parameters from coding are the LPC coefficients ($\{a_k\}$), the long-term prediction lag and gain coefficient (D, β), and the codebook index (i).

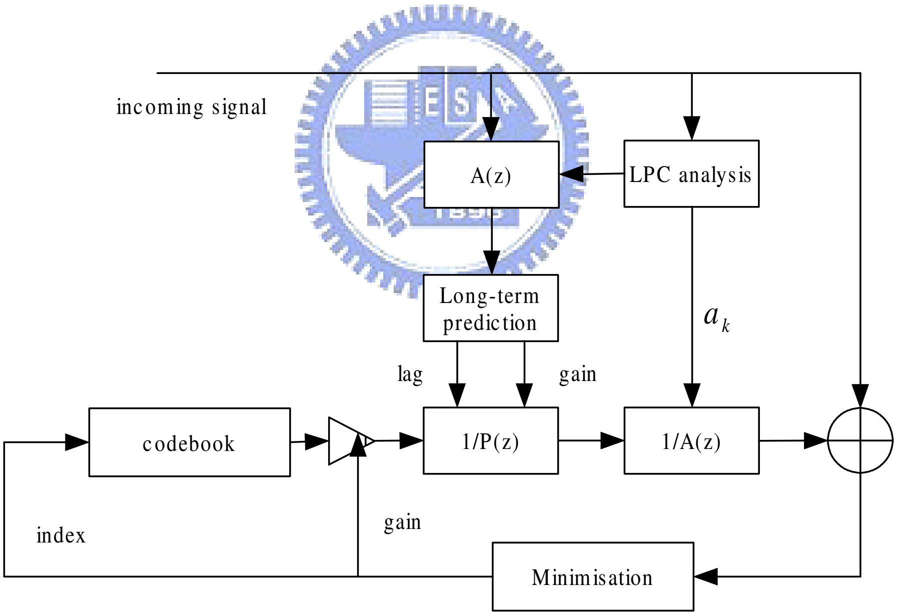

Figure 4.1: CELP coder

4.1.1 Linear Prediction Analysis

One of the most powerful speech analysis techniques is based on linear prediction. This method has become the predominant technique for estimating the basic speech parameters such as the fundamental frequency F_0, vocal tract area functions, and the frequencies and bandwidth of spectral poles and zeros (e.g formants), and for representing speech for low bit rate transmission. The basic idea in linear prediction is that a speech sample is approximated as a linear combination of past speech samples. By minimizing the sum of the squared difference (over a finite interval) between the actual speech samples and the linearly predicted ones, a unique set of predictor coefficients can be determined. For speech, the prediction is done most conveniently in two separate stages: a first prediction based on the short-time spectral envelope of speech known as short-term prediction, and a second prediction based on the periodic nature of the spectral fine structure known as long-term prediction. So , for ECG signals, the same we divide it into two stages: long-term prediction and short-term prediction.

The short-term linear prediction analysis in Fig. 4.2 estimates the all pole filter in each frame, used to generate the spectral envelope of speech signal. The filter typically has $10-12$ coefficients. We have used MATLAB's lpc function to obtain these coefficients however they can be obtained by implementing a lattice filter which acts both as a forward and backward error prediction filter. It gives us reflection coefficients which can be converted to filter coefficients. Levinson-Durbin method can be used effectively to reduce complexity of the filter.

1896

$$\hat{s}(n) = \sum_{i=1}^{p} a_i s(n-i) \tag{4.1}$$

The error between the actual value $s(n)$ and the predicted value $\hat{s}(n)$ is given by:

$$r(n) = s(n) - \hat{s}(n) = s(n) - \sum_{i=1}^{p} a_i s(n-i) \tag{4.2}$$

The error,$r(n)$, is also known as the formant residual signal. Taking the z-transform on both sides, Eq. 4.2 can be written as:

$$R(z) = S(z)[1 - \sum_{i=1}^{p} a_i z^{-i}] \tag{4.3}$$

A signal production model can be defined, where an excitation signal $E(z)$ is passed through a shaping filter,

$$H(z) = \frac{1}{1 - \sum_{i=1}^{p} a_i z^{-i}} \tag{4.4}$$

to produce the reconstructed signal $\hat{S}(z)$. $H(z)$ is the formant synthesis filter and can be interpreted as the frequency response of the vocal tract. $A(z)$ expressed as

$$A(z) = 1 - \sum_{i=1}^{p} a_i z^{-i} = 1 - F(z) \tag{4.5}$$

is the inverse formant filter; its main function is to remove the formants structure from the original signal file.

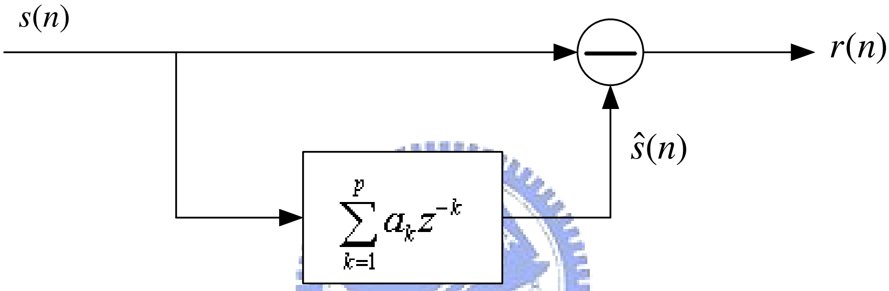

Figure 4.2: Formant prediction.

Linear prediction is optimal in the least-squares sense if the samples of the signal are assumed to be random variables with Gaussian distribution. Experiments have shown that, taken over short time segments, signal samples can be assumed to have a Gaussian distribution. If the prediction system is based on past original samples, we refer to it as forward adapted prediction because the predictor coefficients have to be sent to the receiver as side information. However, if the prediction system is based on past reconstructed samples, we refer to it as backward adaptive prediction and no side information is transmitted because the predictor coefficients can be calculated both at the transmitter and the receiver.

The least-squares method is used in order to determine the Linear Prediction Coefficients (LPC) and is based on minimizing the total squared error with respect to each of the parameters. However, the signal $s(n)$ is not stationary and its statistics are not explicitly known, so it is common practice to consider the ECG signal as stationary over short time intervals.

The residual signal from the formant analysis filter, $A(z)$, still shows pitch periodicity. Another important feature in linear predictive coders is to remove the far-sample redundancy from the original signal. Pitch prediction can be handled by a filter with only one coefficient of the following form:

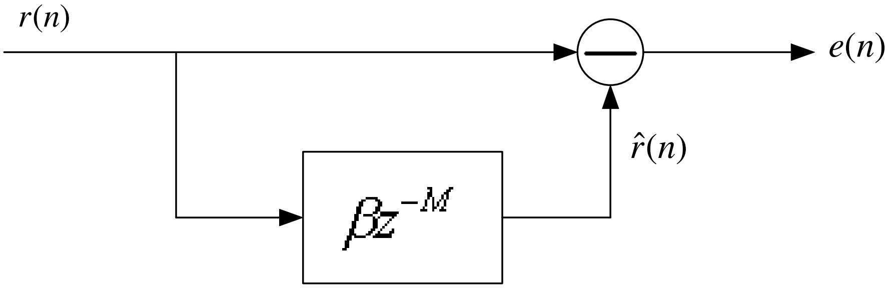

Figure 4.3: Pitch prediction

$$P(z) = \beta z^{-D} \tag{4.6}$$

where β is a scaling factor related to the degree of waveform periodicity and D is the estimated period in samples. This predictor has a time response of a unit sample delayed by M samples; so the pitch predictor estimates that the previous pitch period repeats itself. ECG signals have a pitch in a few hundred hertz. In our implementation we consider pitch frequencies from $350Hz$ to $450Hz$. For $1kHz$ signal these frequencies correspond to pitch delay of 350 samples to 450 samples. For ECG signals, the excitation sequence shows a significant correlation from one pitch period to the next. Therefore, a long-delay correlation filter is used to generate the pitch periodicity in ECG signals as shown in Fig. 4.3. The error signal is

$$e(n) = r(n) - \beta r(n - D) \tag{4.7}$$

and is called the pitch residual signal. Taking the z-transform on both sides, and rearranging the terms, the inverse pitch filter is defined to be

$$B(z) = 1 - \beta z^{-D} \tag{4.8}$$

Its main function is to remove the pitch structure from the original signal. At the decoder stage, the pitch synthesis filter defined as

$$G(z) = \frac{1}{1 - P(z)} \tag{4.9}$$

is excited by the formant residual signal in order to introduce a periodic structure, matching as close as possible that of the original signal.

4.1.2 Line Spectral Frequencies

In order to increase the compression rate, we need to quantize the coefficients using the less bits as possible as we can. It causes the unstability of the filter, so we have used MATLAB's *poly2lsf* function to convert prediction filter coefficients to line spectral frequencies. Line Spectral Frequencies (LSF) is a very popular set for representing the LPC coefficients, because they are related to the speech spectrum characteristics in a straightforward way. The LSF represents the phase angles of an ordered set of poles on the unit circle that describes the spectral shape of the inverse formant filter $A(z)$ defined in Eq.**??** They were first introduced by Itakura in 1975 [19] The main advantages of the LSF are that they can provide easy stability checking procedures, spectral manipulations, and convenient re-conversion to predictor coefficients.

Conversion of the LPC coefficients a_k to the LSF domain relies on the inverse formant filter $A(z)$. Given $A(z)$, its corresponding LSF are defined to be the zeros of the polynomials $P(z)$ and $Q(z)$ defines as :

$$\begin{aligned} A(z) &= 1 + \sum_{k=1}^{p} a_k z^{-k} && (4.10) \\ P(z) &= A(z) - z^{-(p+1)} A(z^{-1}) && (4.11) \\ Q(z) &= A(z) + z^{-(p+1)} A(z^{-1}) && (4.12) \end{aligned}$$

so (4.11) and (4.12) become

$$\begin{aligned} P(z) &= (1-z)(A_0 z^p + A_1 z^{p-1} + \cdots + A_p) && (4.13) \\ Q(z) &= (1+z)(B_0 z^p + B_1 z^{p-1} + \cdots + B_p) && (4.14) \end{aligned}$$

where

$$\begin{aligned} A_0 &= 1 \\ B_0 &= 1 \\ A_k &= (a_k - a_{p+1-k}) + A_{k-1} && (4.15) \\ B_k &= (a_k + a_{p+1-k}) + B_{k-1} && (4.16) \end{aligned}$$

where $k = 1, 2, \cdots, p$ in (4.13) and (4.14) $(1-z)$ and $(1+z)$ are known, so we only need to consider

$$\begin{aligned} P'(z) &= A_0 z^p + A_1 z^{p-1} + \cdots + A_p && (4.17) \\ Q'(z) &= B_0 z^p + B_1 z^{p-1} + \cdots + B_p && (4.18) \end{aligned}$$

using z-transform to transform (4.17) and (4.18) into

$$\begin{aligned} P'(z) &= z^{\frac{p}{2}}[A_0(z^{\frac{p}{2}} + z^{\frac{-p}{2}}) + A_1(z^{\frac{p}{2}-1} + z^{\frac{-p}{2}+1}) + \cdots + A_{\frac{p}{2}}] && (4.19) \\ Q'(z) &= z^{\frac{p}{2}}[B_0(z^{\frac{p}{2}} + z^{\frac{-p}{2}}) + B_1(z^{\frac{p}{2}-1} + z^{\frac{-p}{2}+1}) + \cdots + B_{\frac{p}{2}}] && (4.20) \end{aligned}$$

If $A(z)$ is minimum phase, all the roots of $P(z)$ and $Q(z)$ will lie on the unit circle, alternating between the two polynomials with increasing frequency. The roots occur in complex conjugate pairs and hence there are p LSF lying between 0 and π. The value of the LSF can be converted to Hertz (Hz) by multiplying by the factor $F_s/2/pi$ where F_s is the sampling frequency. Another important characteristic about the LSF is the localized spectral sensitivity. For the predictor coefficients, a small distortion in one coefficient could dramatically distort the spectral shape and even lead to an unstable synthesis filter. Whereas, if one the LSF is distorted, the spectral distortion occurs only in the neighborhood of the modified LSF.

In many LPC coders, the LPC filtering is carried out by interpolating the predictor coefficients between two successive analysis frames into a subframe level such that a smoother transition is achieved. The interpolation can be performed in the LSF domain to guarantee the stability of the resulting filters.

4.1.3 Codebook Generation

Vector Quantization (VQ) [20] has been widely known for its excellent rate-distortion performance. It may be simply viewed as a form of pattern recognition or matching where an input pattern is 'approximated' by one standard template of a predetermined codebook. Conceivably, a good vector quantizer is subject to a good codebook. The most commonly used method for designing a VQ codebook is the LBG algorithm [20]. It is an iterative method and involves creating a primitive seed of letter reference from which an improving alphabet evolves step by step. The performance of the overall codebook depends on the selection of the initial seed (codebook). This initial seed could be a code generated arbitrarily or adopted previously. Nevertheless, the almost exclusively adopted method is called the splitting algorithm[20], which grows increasingly larger codebooks of a fixed dimension from the lowest resolution codebook of a training set to the codebook of size as required for the initial seed. And, the simplest but less reliable initialization is by means of the so-called random guess method [20].

In 1980, Linde, Buzo, and Gray (LBG) proposed a VQ design algorithm based on a training sequence. The use of a training sequence bypasses the need for multi-dimensional integration. A VQ that is designed using this algorithm are referred to in the literature as an LBG-VQ. A VQ is nothing more than an approximator. The idea is similar to that of "rounding-off" (say to the nearest integer). An example of a 1-dimensional VQ is shown in Fig.4.4: Here, every number less than -2 are approximated by -3. Every number between -2 and 0 are approximated by -1. Every number between

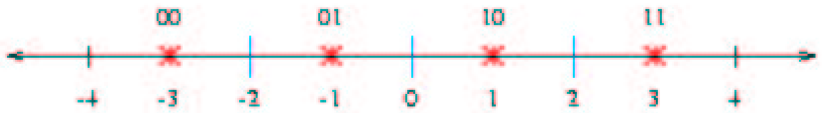

Figure 4.4: One dimensional VQ

0 and 2 are approximated by +1. Every number greater than 2 are approximated by +3. Note that the approximate values are uniquely represented by 2 bits. This is a 1-dimensional, 2-bit VQ. It has a rate of 2 bits/dimension. An example of a 2-dimensional VQ is shown in Fig.4.5: Here, every pair of numbers falling in a particular region are

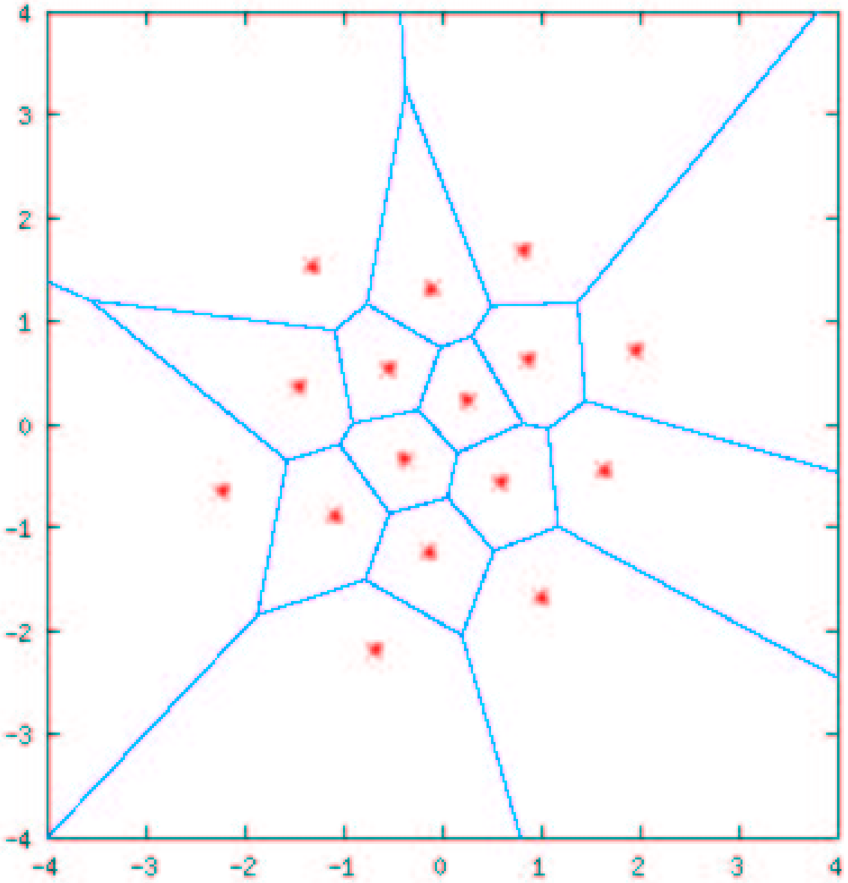

Figure 4.5: Two dimensional VQ

approximated by a red star associated with that region. Note that there are 16 regions and 16 red stars–each of which can be uniquely represented by 4 bits. Thus, this is a 2-dimensional, 4-bit VQ. Its rate is also 2 bits/dimension. In the above two examples, the red stars are called codevectors and the regions defined by the blue borders are called encoding regions. The set of all codevectors is called the codebook and the set of all encoding regions is called the partition of the space.

We assume that there is a training sequence consisting of M source vectors: $\tau = \{x_1, x_2, \cdots, x_M\}$. This training sequence can be obtained from some large database. For example, if the source is a speech signal, then the training sequence can be obtained by recording several long telephone conversations. M is assumed to be sufficiently large so that all the statistical properties of the source are captured by the training sequence. We assume that the source vectors are k-dimensional, e.g. $x_m = (x_{m,1}, x_{m,2}, \cdots, x_{m,k})$, where $m = 1, 2, \cdots, M$. Let N be the number of codevectors and let $C = \{c_1, c_2, \cdots, c_N\}$, represents the codebook. Each codevector is k-dimensional, e.g., $c_n = (c_{n,1}, c_{n,2}, \cdots, c_{n,k})$ where $n = 1, 2, \cdots, N$. Let S_n be the encoding region associated with codevector c_n and let $P = \{S_1, S_2, \cdots, S_N\}$ denote the partition of the space. If the source vector x_m is in the encoding region S_n, then its approximation (denoted by $Q(x_m)$) is c_n: $Q(x_m) = c_n$, if $x_m \in S_n$. Assuming a squared-error distortion measure, the average distortion is given by:

$$D_{ave} = \frac{1}{Mk} \sum_{m=1}^{M} \|x_m - Q(x_m)\|^2 \tag{4.21}$$

LBG Design Algorithm is as follows:

1. Given τ. Fixed $\epsilon > 0$ to be a small number.

2. Let $N = 1$ and

$$c_1^* = \frac{1}{M} \sum_{m=1}^{M} x_m. \tag{4.22}$$

Calculate

$$D_{ave}^* = \frac{1}{Mk} \sum_{m=1}^{M} \|x_m - c_1^*\|. \tag{4.23}$$

3. Splitting: For $i = 1, 2, \cdots, N$, set

$$\begin{aligned} c_i^0 &= (1+\epsilon)c_i^* \qquad (4.24) \\ c_{N+i}^0 &= (1-\epsilon)c_i^* \qquad (4.25) \end{aligned}$$

   Set $N = 2N$

4. Iteration: $D_{ave}^0 = D_{ave}^*$. Set the iteration index $i = 0$

   (a) For $m = 1, 2, \cdots, M$, find the minimum value of

   $$\|x_m - c_n^{(i)}\|^2, \tag{4.26}$$

   over all $n = 1, 2, \cdots, N$. Let n^* be the index which achieves the minimum. Set

   $$Q(x_m) = c_{n^*}^{(i)}. \tag{4.27}$$

   (b) For $n = 1, 2, \cdots, N$, update the codevector

   $$c_n^{i+1} = \frac{\sum_{Q(x_m)=c_n^i} x_m}{\sum_{Q(x_m)=c_n^i} 1} \tag{4.28}$$

   (c) Set $i = i + 1$

   (d) Calculate

   $$D_{ave}^i = \frac{1}{Mk} \sum_{m=1}^{M} \|x_m - Q(x_m)\|^2 \tag{4.29}$$

   (e) If $D_{ave}^{i-1} - D_{ave}^i / D_{ave}^{i-1} > \epsilon$, go back to Step 4a.

   (f) Set $D_{ave}^* = D_{ave}^i$. For $n = 1, 2, \cdots, N$, set $c_n^* = c_n^i$ as the final codevectors.

5. Repeat Steps 3 and 4 until the desired number of codevectors is obtained.

1896

4.2 Using the Idea of AMR-WB for Compression of ECG Signals

The proposed coder is based on the algebraic code excited linear prediction (ACELP) structure for signal compression. ACELP is a parametric coder; the basic parts comprise an excitation signal drawn from a codebook (a collection of codevectors) and shaped through a long term predictor and an AR filter (LPC model), synthesizing the output signal. The parameters are calculated in an analysis-by-synthesis fashion: the long-term and short-term filters ($l/P(z)$ and $l/A(z)$) are determined from the incoming signal, and the best codevector (in an MSE sense) is found through filtering, comparison, and selection. The block diagrams of the encoding and decoding algorithms are shown in Fig. 4.6 and Fig. 4.7, respectively.

4.2.1 Encoder

Coding is performed in blocks of 1 s frame. The codec is based on the ACELP coding model. The ECG input signal is pre-processed using a pre-emphasis filter of the form $H_{pre-emph}(z) = 1 - \mu z^{-1}$ with $\mu = 0.68$. The ACELP model is then applied to the pre-emphasized signal. The long-term, or pitch, synthesis filter is usually given by

$$\frac{1}{P(z)} = \frac{1}{1 - g_p z^{-T}} \tag{4.30}$$

where T is the pitch delay and g_p is the pitch gain. The pitch lag is encoded with 7 bits per frame. The pitch gain is quantized using 10 bits per frame. Open-loop pitch analysis is performed once per (each 1 s) to find the estimate of the pitch lag in each frame. This is done in order to simplify the pitch analysis. Open-loop pitch estimation is based on the ECG signal $s(n)$. The open-loop pitch analysis is performed as follows. First, the Average Magnitude Difference Function (AMDF) algorithm for the ECG signal is determined for each pitch lag value d by:

$$AMDF(d) = \frac{1}{434} \sum_{n=1}^{434} |s(n) - s(n+d)|, \qquad d = 350, \cdots, 434 \tag{4.31}$$

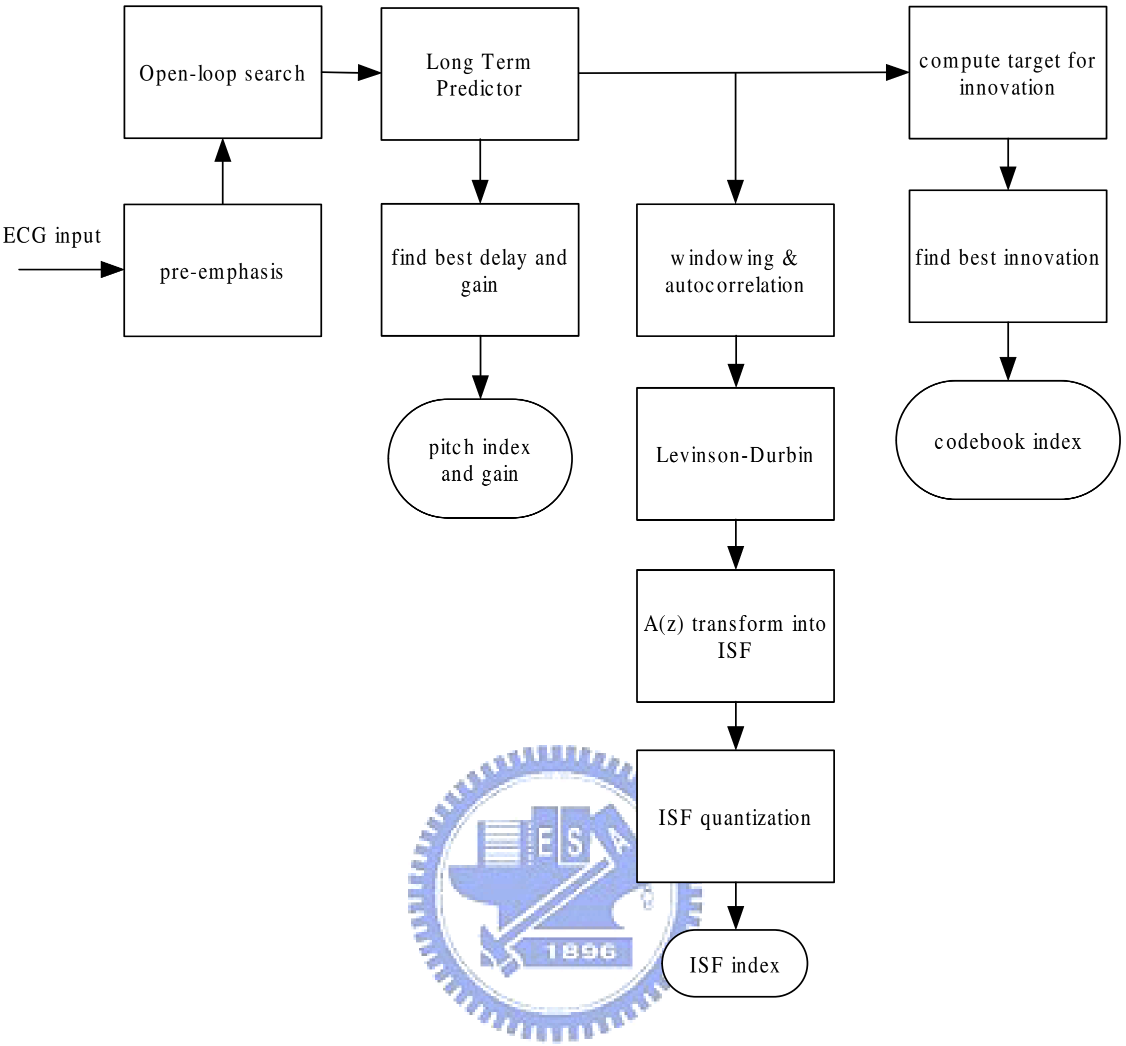

Figure 4.6: Detailed block diagram of the encoder

The estimated pitch-lag is the delay that minimizes the $AMDF(d)$ function. The open loop gain is given by

$$g_p = \frac{\sum_{n=350}^{434} s(n)s(n-d_{max})}{\sqrt{\sum_{n=350}^{434} s^2(n) \sum_{n=350}^{434} s^2(n-d_{max})}} \tag{4.32}$$

where d_{max} is the pitch delay that minimizes $AMDF(d)$.

An 8th order linear prediction (LP), or short-term, synthesis filter is usually given by

$$\hat{A}(z) = 1 + \sum_{i=1}^{m} \hat{a}_i z^{-i} \tag{4.33}$$

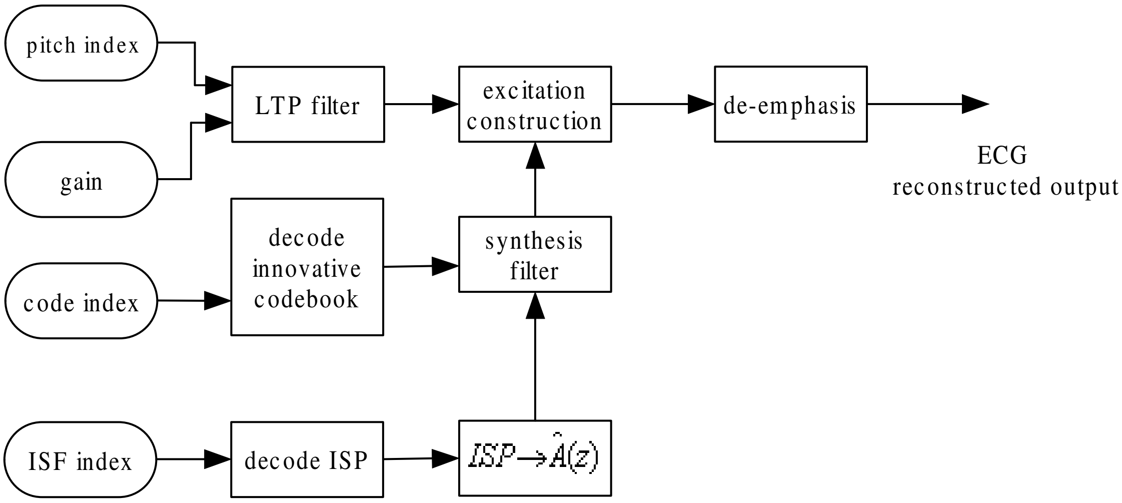

Figure 4.7: Detailed block diagram of the decoder

where $\hat{a}_i, i = 1, \cdots, m$ are the quantized linear prediction (LP) parameters, and $m = 8$ is the predictor order. Linear Prediction (LP) analysis is performed once per 1s frame. The autocorrelations of ECG signals are converted to the LP coefficients using the Levinson-Durbin algorithm. The autocorrelations are used to obtain the LP filter coefficients $a_k, k = 1, \cdots, 8$ by solving the set of equations.

$$\sum_{i=1}^{8} a_k r(\|i - k\|) = -r(i) \tag{4.34}$$

where $i = 1, \cdots, 8$. The set of equation in (4.34) is solved using the Levinson-Durbin algorithm. This algorithm uses the following recursion:

$$
\begin{aligned}
E(0) &= r(0) \\
For \quad i &= \quad 1 \quad to \quad 8 \quad do \\
k_i &= -\left[r(i) + \sum_{j=1}^{i-1} a_j^{i-1} r(i-j) \right] / E(i-1) \\
a_i^{(i)} &= k_i \\
For \quad j &= 1 \quad to \quad i-1 \quad do \\
a_j^{(i)} &= a_j^{(i-1)} + k_i a_{i-j}^{(i-1)} \\
E(i) &= (1-k_i^2)E(i-1)
\end{aligned}
$$

The final solution is given as $a_j = a_j^8$, $j = 1, \cdots, 8$ Then the LP coefficients are transformed to immittance spectrum pairs (ISP) [19] domain for quantization purposes.

4.2.2 Decoder

The received bits of the quantized ISP are used to reconstruct the ISP vector and to convert to LP filter coefficient a_k, which is used for synthesizing ECG signals in the frame. Then in each frame, the received codebook index is used to extract the positions and to find the excitation $c(n)$. The excitation signals, $c(n)$, are applied into the synthesis filter

$$H(z) = \frac{1}{\hat{A}(z)} = \frac{1}{1 + \sum_{i=1}^{m} \hat{a}_i z^{-i}} \tag{4.35}$$

to obtain the linear predictive ECG signals. In each frame, the received pitch index is is used to find the integer part of the pitch lag M, and the pitch gain bits to reconstruct $\hat{g}_p$. The long term predictor could be reconstructed ,

$$\frac{1}{\hat{P}(z)} = \frac{1}{\hat{g}_p z^{-M}} \tag{4.36}$$

, the total excitation is given by

$$\hat{U}(z) = c(z)H(z)/\hat{P}(z) \tag{4.37}$$

Finally, the total excitation is de-emphasized using the filter

$$H_{de-emph}(z) = \frac{1}{1 - \mu z^{-1}} \tag{4.38}$$

So the output signals become

$$\hat{s}(z) = H_{de-emph}(z)\hat{U}(z) \tag{4.39}$$

4.2.3 Simulation Results

The results show the high efficiency of this method for ECG compression. By this method, we achieved the CR about 30 with a very good reconstruction quality. Table 4.1 lists the CR and PRD values for some other compression methods. It shows that Adaptive Multi-Rate Wideband codec method has very better results. Adaptive Multi-Rate Wideband codec is a very computationally simple algorithm and is easy to implement, in comparison with many complex coding methods.

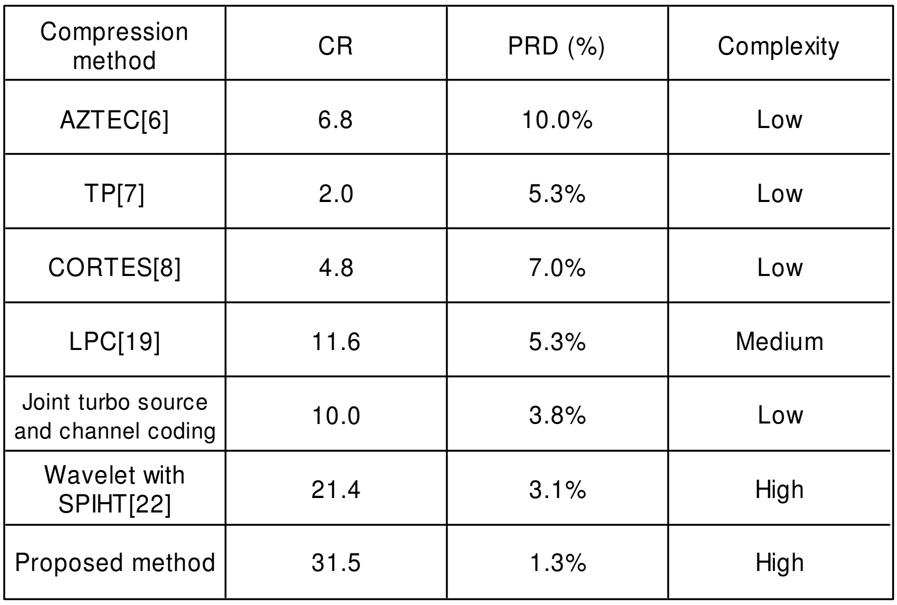

Compression method	CR	PRD (%)	Complexity
AZTEC[6]	6.8	10.0%	Low
TP[7]	2.0	5.3%	Low
CORTES[8]	4.8	7.0%	Low
LPC[19]	11.6	5.3%	Medium
Joint turbo source and channel coding	10.0	3.8%	Low
Wavelet with SPIHT[22]	21.4	3.1%	High
Proposed method	31.5	1.3%	High

Table 4.1: Compression performance for ECG signals database with different compression methods

The original signal, reconstructed signal and error between them for three records with the corresponding CR and PRD values are shown in Figs. 4.8, 4.9 and 4.10.

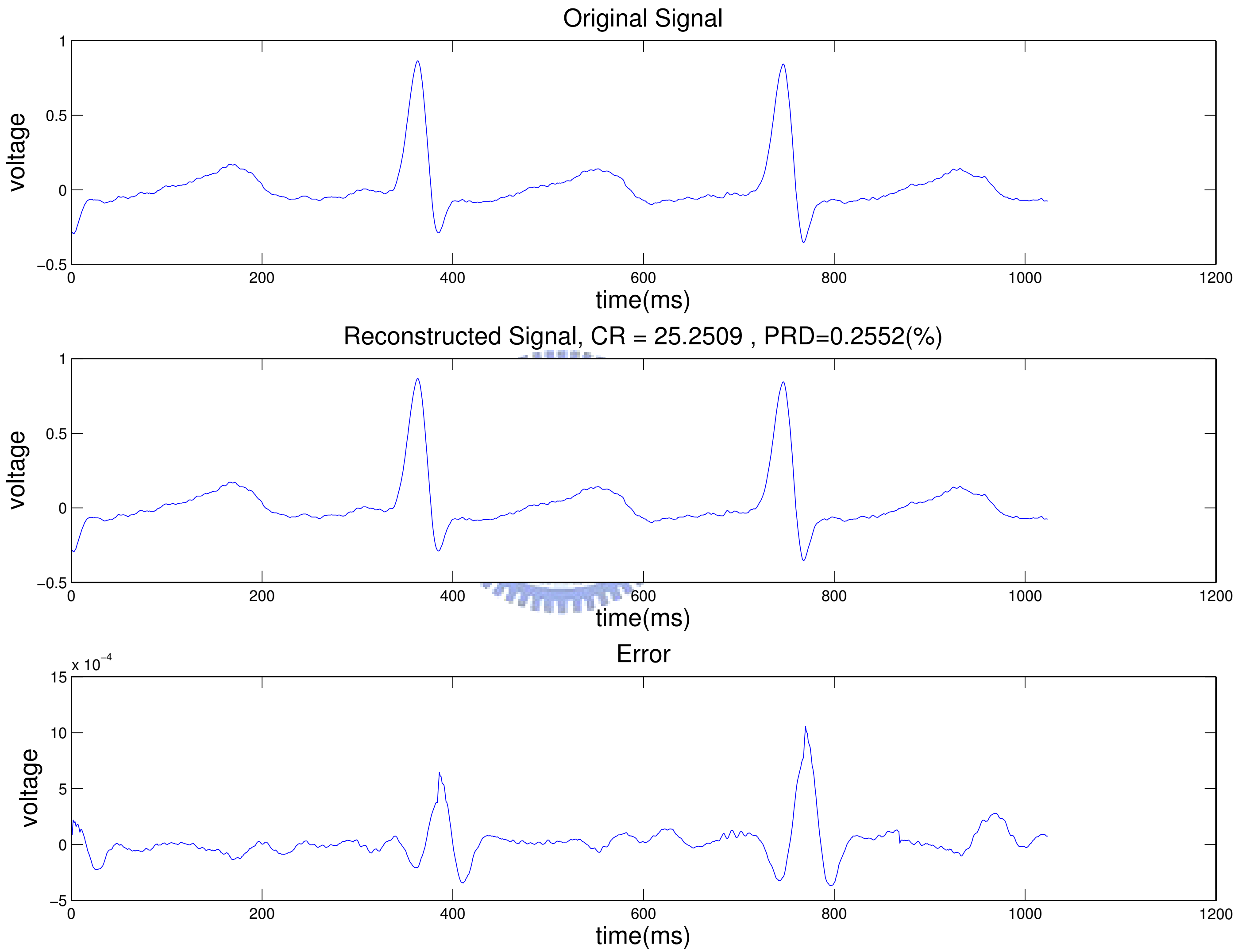

Figure 4.8: ECG compression performance using the adaptive multi-rate wideband codec method

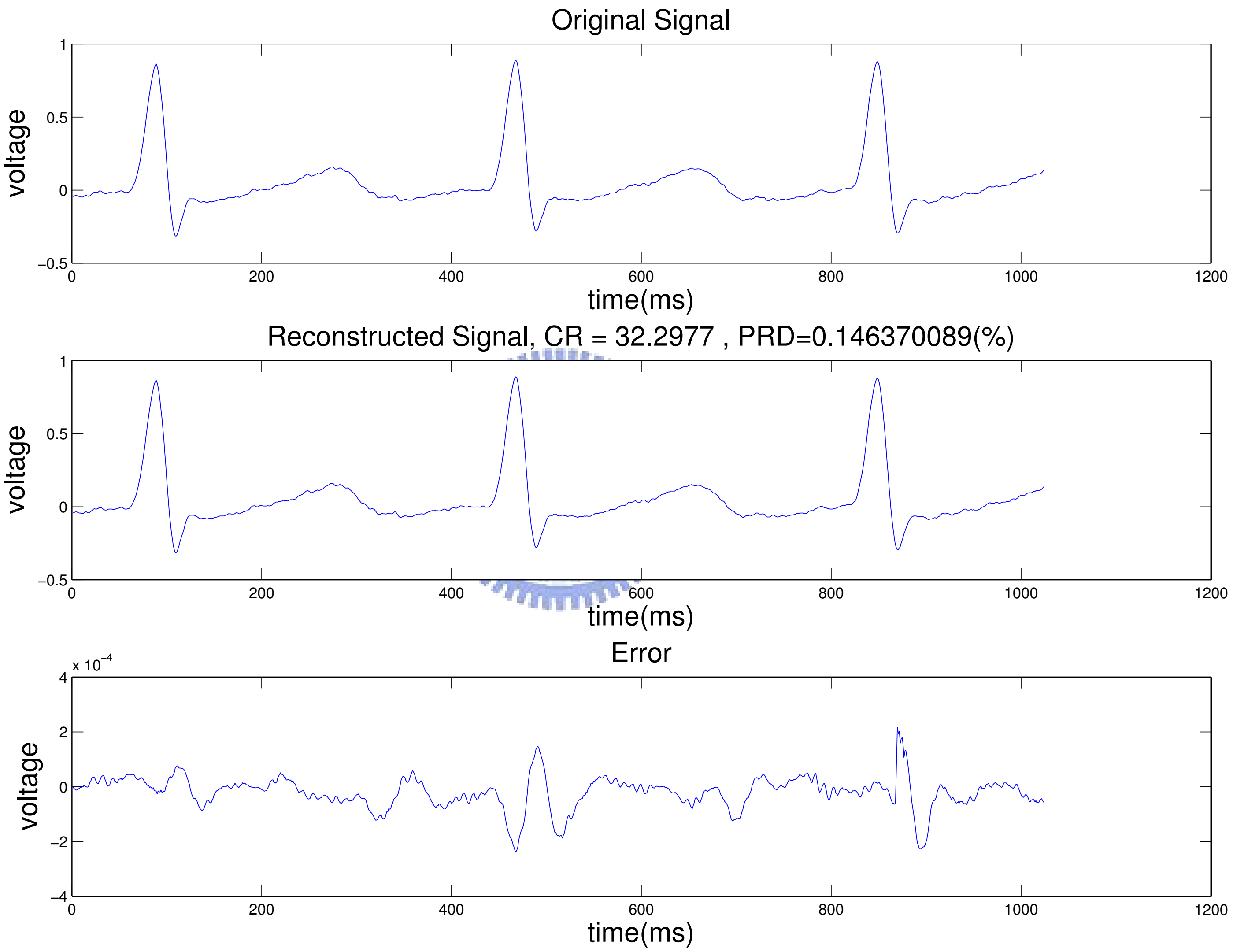

Figure 4.9: ECG compression performance using the adaptive multi-rate wideband codec method

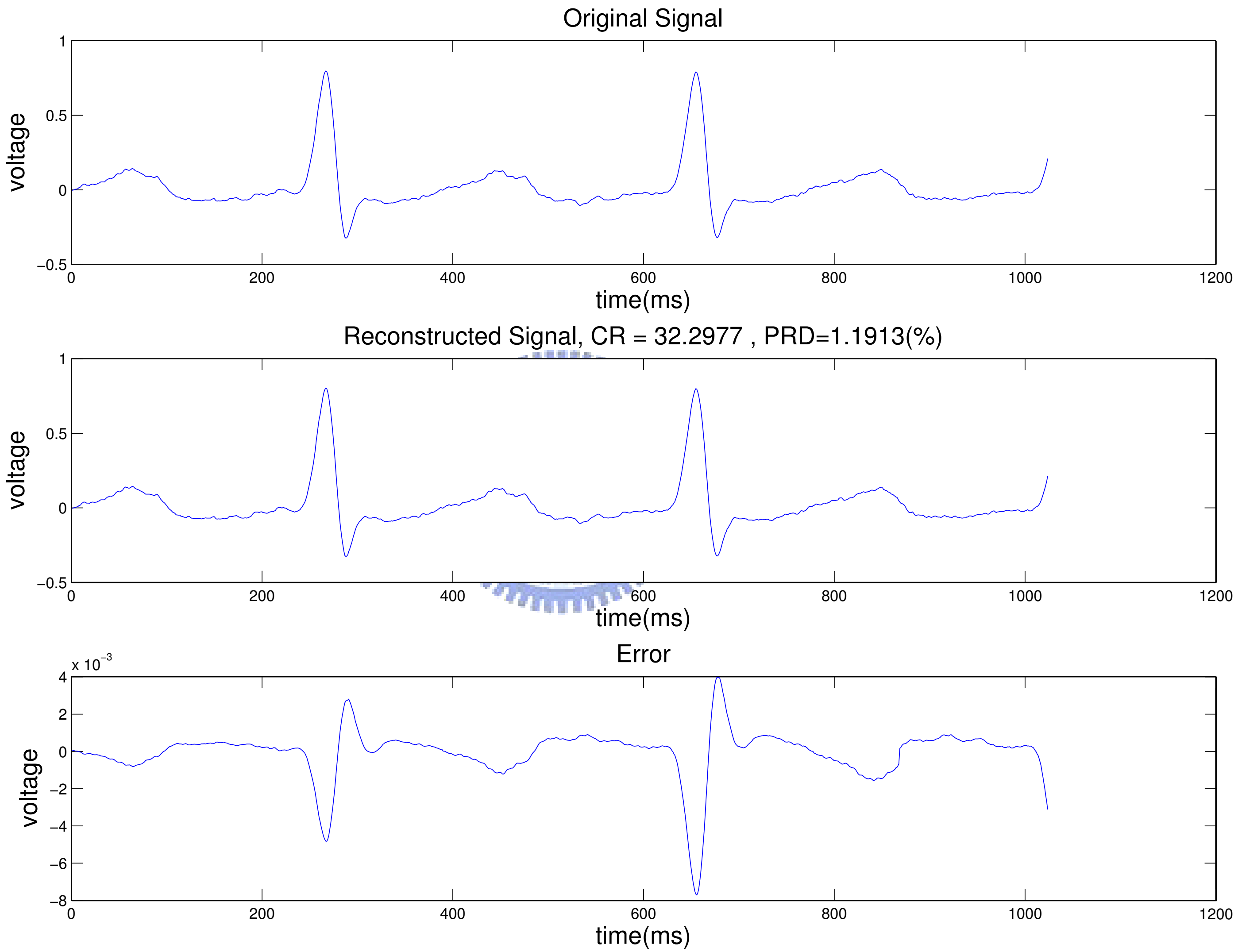

Original Signal

Reconstructed Signal, CR = 32.2977 , PRD=1.1913(%)

Error

Figure 4.10: ECG compression performance using the adaptive multi-rate wideband codec method

Chapter 5

Conclusion

We present a lossless turbo source coding scheme and its extension for joint source and channel coding of ECG data. The turbo source coding scheme guarantees lossless recovery of the source information through a decremental redundancy loop in the encoder. The coding system is very flexible and is adaptive in nature. According to the feedback receiver measurement the transmitter adjust its redundancy ratio to match the channel condition. The compression ratio of our scheme is higher than most existing ECG compression schemes and the joint source-channel coding approach simplify the transceiver architecture and provides excellent wireless transmission performance. We also found the optimal (in terms of complexity) DCT block size is about one normal beat. Larger block sizes do not provide noticeable performance improvement.

We modify the Adaptive Multi-Rate Wideband codec, which was originally designed for speech coding, for lossy ECG data compression and prove that outstanding compression performance is achievable, achieving a compression ratio about 30 with a very good reconstruction quality. The resolutions of the transmitted parameters and the code book size can be adjusted to achieve the desired PRD. The repeating (regular) parts of the waveform are effectively compressed, while irregularities are represented with a high degree of accuracy. Although very impressive compression performance is obtained, we believe that through more refined parameter optimization, source coders with a better ratio of signal quality-to-bit-rate can be obtained.

1896

Bibliography

[1] G. Caire, S. Shamai, and S. Verdú, "A new data compression algorithm fo sources with memory based on error correcting codes," in *Proc. IEEE Information Theory Workshop*, pp. 291-295, Paris, France, Apr. 2003.

[2] G. Caire, S. Shamai, and S. Verdú, "Universal data compression with LDPC codes," in *Proc. International Symposium on Turbo Codes and Related Topics*, Brest, France, pp. 55-58, Sep. 2003.

[3] J. Garcia-Frias and Y. Zhao, "Compression of binary memoryless sources using punctured turbo codes," *IEEE Communications Letters*, vol. 6, no. 9, pp. 394-396, Sep. 2002.

[4] J. Hagenauer, J. Barros, and A. Schaefer, "Lossless turbo source coding with decremental redundancy," in *Proc. International ITG Conference on Source and Channel Coding*, Erlangen, Germany, pp. 333-339, Jan. 2004.

[5] N. Dütsch, J. Hagenauer, "Combined incremental and decremental redundancy in joint source-channel coding," in *Proc. International Symp. Information Theory and its Applications*, Parma, Italy, pp. 775-779, Oct. 2004.

[6] J . R. Cox, F. M. Nolle, H. A. Fozzard, and G. C. Oliver, "AZTEC, a preprocessing program for real-time ECG rhythm analysis," *IEEE Trans. Biomed. Eng.*, vol. BME-15, pp. 128-129, Apr. 1968.

[7] W. C. Mueller, ”Arrhythmia detection program for an ambulatory ECG monitor, ” *Biomed. Sci. Instrument.*, vol. 14, pp. 81-85, 1978

[8] J . P. Abenstein and W. J . Tompkins, “New data-reduction algorithm for real-time ECG analysis,” *IEEE Trans. Biomed. Eng.*, vol. BME-29, pp. 43-48, Jan. 1982.

[9] W. J. Tompkins and J . G. Webster, *eds.*, *Design of microcompurer-based medical Instrumentation,* Englewood Cliffs, NJ: Prentice-Hall, 1981.

[10] R. C. Barr, S . M. Blanchard, and D. A. Dipersio, “SAPA-2 is the Fan,” *lEEE Trans. Biomed. Eng.*, vol. BME-32, p. 337, May 1985.

[11] C. Berrou, A. Glavieux, and P. Thitimajshima, “Near shannon limit errorVcorrecting coding and decoding: Turbo-codes,” in *Proc. IEEE ICC,* (Geneva, Switzerland), pp. 1064-1070, May 1993.

[12] J. Hagenauer, “The turbo principle-tutorial introduction and state of the art” in *Proc. Int. Symp. Turbo Codes and Related Topics,* (Brest, France), pp. 1-11, 1997.

[13] J. Garcia-Frias and Y. Zhao, “Compression of binary memoryles sources using punctured turbo codes,” *IEEE Commun. Lett.,* pp. 394-396, 2002.

[14] J. Hagenauer, ”Source-controlled channel decoding,” *IEEE Trans. Commun.*, vol. 43, pp. 2449-2457, Sep. 1995.

[15] J. Hagenauer, E. Offer, and L. Papke, “Iterative decoding of binary block and convolutional codes,” *IEEE Trans. Inform. Theory,* pp. 429-445, Mar. 1996.

[16] A. A. Petrosian “Optimal zonal coding of digital Signals with transform,” *Problemi Peredachi Inforinatsii*, Vol. 27, No. 2, pp. 46-58, Moscow, Nauka, (in Russian. Translated into English in: *Problems of Information Transmission,*27-2, pp. 128-140, Oct. 91, New York, Plenum Publishing Corp.).

[17] R. Bellman, S. E. Dreyfus, *Applied Dynamic Programming. Princeton University Press,*, Princeton, NJ, 1962.

[18] B. S. Atal, “Code-excited linear prediction (CELP): High quality speech at very low bit rates,” in *Proc. Int. Conf. Acoust. Speech, signal Proc.*, pp. 937-940, 1985.

[19] F. Itakura, “Line Spectrum Representation of Line Predictive Coefficients,” J. Acoust. Soc. Am. 57 Supplement(1), pp. S.35 (1975)

[20] A.Gersho and R.M Gray, “Vector quantization and signal compression,” Kluwer Academic, 1992.

[21] A. Al-Shrouf, M. Abo-Zahhad, S. M. Ahmed, “A novel compression algorithm for electrocardiogram signals based on the linear prediction of the wavelet coefficients,” *Digital Signal Processing,* vol. 13, no. 4, pp. 604-622, Oct. 2003.

[22] M. Pooyan, A. Taheri, M. Moazami-Goudarzi, I. Saboori, “Wavelet Compression of ECG Signals Using SPIHT Algorithm,” *Trans. Engineering, Computing and Technology*, vol. 2, Dec. 2004.

1896

誌謝

首先感謝我的指導教授 蘇育德博士這二年來不只在研究上的敦敦教誨，使得論文能更加順利的完成，讓我在通訊領域上有更加深入的了解。並且在人生的道路上給我適時的指引讓我不致於迷失人生的方向。感謝口試委員蘇賜麟教授，陳儒雅教授以及許大山教授給予的寶貴意見，以補足這份論文上的缺失與不足之處。另外也要感謝實驗室的學長姐、同學及學弟妹的幫忙還有鼓勵，讓我不僅在學習的過程中獲益匪淺，同時也爲這二年的生活增添了許多歡樂。

最後，我更要感謝一直關心我、鼓勵我的家人，沒有他們在背後的支持我無法這麼順利的完成論文，謹獻上此論文，代表我最深的敬意！

作者簡歷

施泓瑋，台北縣新莊市人，1982 年生

國立新莊高級中學	1997.9～2000.6
國立交通大學電信工程學系	2000.9～2004.6
國立交通大學電信工程學系系統組	2004.9～2006.6

Graduate Course:

1. Coding Theory
2. Digital Communications
3. Random Process
4. Digital Signal Processing
5. Detection and Estimation Theory
6. Optimization
7. Adaptive Signal Processing
8. Special Topics in Digital Signal Processing
9. Special Topics in Communication Systems
10. Queuing Theory